International Journal of Coal Geology 94 (2012) 250–270

Contents lists available at ScienceDirect

International Journal of Coal Geology

journal homepage: www.elsevier.com/locate/ijcoalgeo

Mineralogical and geochemical compositions of the Pennsylvanian coal in the Adaohai Mine, Daqingshan Coalfield, Inner Mongolia, China: Modes of occurrence and origin of diaspore, gorceixite, and ammonian illite

Shifeng Dai [a,*], Jianhua Zou [a,b], Yaofa Jiang [c], Colin R. Ward [d], Xibo Wang [a], Tian Li [a], Weifeng Xue [a], Shande Liu [a], Heming Tian [a], Xinhao Sun [a], Dao Zhou [a]

[a] State Key Laboratory of Coal Resources and Safe Mining, China University of Mining and Technology, Beijing 100083, China
[b] Chongqing Institute of Geology and Mineral Resources, Chongqing 400042, China
[c] Xuzhou Institute of Architectural Technology, Xuzhou 221116, China
[d] School of Biological, Earth and Environmental Sciences, University of New South Wales, Sydney, NSW 2052, Australia

ARTICLE INFO

Article history:
Received 14 April 2011
Received in revised form 13 June 2011
Accepted 15 June 2011
Available online 29 June 2011

Keywords:
Minerals in coal
Elements in coal
Diaspore
Gorceixite
Ammonian illite

ABSTRACT

Aluminum-hydroxide (boehmite)-rich Pennsylvanian coals of high volatile A bituminous rank were found previously in the Jungar Coalfield, Inner Mongolia, China. This paper reports new results on 48 bench samples of the CP2 coal from the adjacent Adaohai Mine, Daqingshan Coalfield, Inner Mongolia, and provides new insights into the origin and modes of occurrence of the minerals and elements present in the CP2 coal.

Compared to the same coal in the adjacent mines, the CP2 coal in the Adaohai Mine has a higher rank ($R_{o,\,ran}$ = 1.58%), which is attributed to igneous intrusions during the Late Jurassic and Early Cretaceous Epochs. The proportion of inertinite (35.3%) in the coal is higher than that in other Late Paleozoic coals in northern China but lower than that in the Jungar coals.

Minerals in the CP2 coal include diaspore, boehmite, gorceixite, calcite, dolomite, siderite, clay minerals (kaolinite and ammonian illite), and trace amounts of anatase, fluorapatite, quartz, and pyrite. Based on mineral proportions in the coal bench samples, the CP2 coal may be divided into four Zones (I to IV) from bottom to top. The major mineral in Zones I and IV is kaolinite. Zones II and III are mainly composed of ammonian illite, diaspore, boehmite, gorceixite, calcite, dolomite, and siderite. Diaspore-, boehmite-, and gorceixite-forming materials were derived from oxidized bauxite in the weathered crust of the Benxi Formation in the sediment-source region during peat accumulation. However, gorceixite may have formed earlier than diaspore; the diaspore was derived from gibbsite that was subjected to dehydration by the heat of the igneous intrusions. The ammonian illite may have been formed at a relatively high temperature by interaction of kaolinite with nitrogen released from the organic matter in the coal during metamorphism caused by the igneous intrusion. The calcite and dolomite occur as epigenetic cell- and fracture-fillings and were probably derived from the igneous fluids.

Compared to the common Chinese and world coals, the CP2 coal is enriched in CaO (1.69%), MgO (0.32%), P_2O_5 (0.214%), F (207 μg/g), Ga (16.3 μg/g), Zr (446 μg/g), Ba (276 μg/g), Hg (0.33 μg/g), and Th (12.4 μg/g), but has a lower SiO_2/Al_2O_3 ratio due to the higher proportions of diaspore, boehmite, and gorceixite in the coal. The F occurs mainly in gorceixite and fluorapatite. The major carriers of Ga are diaspore and kaolinite but not gorceixite. Barium mainly occurs in gorceixite and barite. Mercury was probably derived from the igneous intrusion and is distributed in both the organic matter and the minerals. The elements are classified into five associations by cluster analysis, Groups A, B, C, D, and E. Group A represents a REE-Be-Y-Se-Ga-Ge-Sc-In-Pb-Bi-Nb-Ta-TiO_2-W-Hg-Sb-Zr-Hf-Th-U association. Most of the elements in Group A are lithophile elements that occur in aluminosilicate minerals. Group B (Sn-Te-Zn-Cd-V-As-Cr-Cu-Mo-Ni-Re) is weakly correlated with ash yield and is associated with unidentified trace sulfide minerals. Elements in Group C (A_d-Na_2O-Al_2O_3-SiO_2- Li-K_2O-Rb-Cs-Tl association) probably occur in the clay minerals and diaspore. Group D consists of P_2O_5, Ba, F, Sr, S, and Cl, and with the exception of S, they occur in minerals (gorceixite and fluorapatite). Oxides of Fe_2O_3-MnO-CaO-MgO make up Group E and mainly occur in the carbonate minerals. The coals are enriched in light REEs and the LREEs–HREEs have been highly fractionated, with an average $(La/Yb)_N$ of 8.71. The heavy REEs in the coals have a stronger organic affinity than the LREEs.

* Corresponding author at: State Key Laboratory of Coal Resources and Safe Mining, China University of Mining and Technology, D11, Xueyuan Road, Haidian District, Beijing 100083, China. Tel./fax: +86 10 62341868.
E-mail address: daishifeng@gmail.com (S. Dai).

0166-5162/$ – see front matter © 2011 Elsevier B.V. All rights reserved.
doi:10.1016/j.coal.2011.06.010

1. Introduction

Mineral matter in coal consists of discrete mineral particles, inorganic elements incorporated within the organic compounds, dissolved salts and other inorganic substances in the coal's pore water (Ward, 2002). In addition to the common minerals in coal, including quartz, clay minerals (especially kaolinite, illite, and mixed-layer illite-smectite), carbonates (e.g., siderite, calcite, and dolomite), and sulfide minerals (e.g., pyrite and marcasite) (Harvey and Ruch, 1986; Mackowsky, 1968; Palmer and Lyons, 1996; Ward, 1978), minor but sometimes significant accessories have been identified in coal (Belkin et al., 2010; Bouška et al., 2000; Cressey and Cressey, 1988; Dewison, 1989; Finkelman and Stanton, 1978; Kalaitzidis et al., 2010; Koukouzas et al., 2010; Loughnan and Goldbery, 1972; Rao and Walsh, 1997; Wang, 2009; Ward, 1974; Ward et al., 1996).

Minor minerals of aluminum-hydroxides, including boehmite and diaspore, have been identified in some coals (Dai et al., 2006, 2008, 2010; Kalkreuth et al., 2010; Wang et al., 2011a,b; Ward, 2002). Understanding the concentrations and origins of Al-hydroxide minerals in coal is significant both geochemically and practically, because hydroxide minerals in coal may not only serve as an indicator of mineralization and paleoclimate (Cheng et al., 2001; Dai et al., 2006; Wang, 1982), but are also the major carriers of valuable elements Al and Ga that could be potentially recovered from associated combustion residues (fly ashes) (Dai et al., 2008, 2011; Seredin and Finkelman, 2008; Seredin and Shpirt, 1995). The high proportion of boehmite in the coals from the Jungar Coalfield, Inner Mongolia, northern China, was derived from its proximity to an Al-rich sediment source region (Dai et al., 2006, 2008). The management of the Heidaigou Surface Mine in the Jungar Coalfield, which is owned by Shenhua Group Jungar Energy Corporation Ltd., has built a pilot plant to develop technologies to extract the metals from combustion residues.

The Daqingshan Coalfield is situated to the north of and close to the Jungar Coalfield (Fig. 1A), and is closer to the sediment source region than the Jungar field. This paper reports new data on the mineralogy and geochemistry of the CP2 coal in the Adaohai Mine of the Daqingshan Coalfield. Special emphasis is placed on the modes of occurrence and origin of abundant diaspore, gorceixite, and ammonian illite in the coal.

2. Geological setting

The Daqingshan Coalfield is located in Inner Mongolia of northern China, covering the area of north latitude 40°35′–40°44′ and east longitude 110°07′–110°31′. It includes 16 mines distributed from west to east (Fig. 1B), with the Adaohai Mine being located in the southeast of the coalfield (Fig. 1B).

The coal-bearing strata in the Daqingshan Coalfield include the Pennsylvanian Shuanmazhuang Formation and the Early Permian Zahuaigou Formation (Jia and Wu, 1995; Wang and Ge, 2007; Zhang et al., 2000; Zhong et al., 1995; Zhou and Jia, 2000). They were deposited in a continental environment (Fig. 2).

The major coalbed in the Daqingshan Coalfield is the CP2 coal, which is located in the upper portion of the Shuanmazhuang Formation. The thickness of the coalbed varies from 4.72 to 42.79 m and averages 22.58 m. The CP2 coal contains 3 to 42 parting layers with thickness from 0.02 to 3.4 m. As a result of epigenetic tectonic movements, the CP2 coal was strongly brecciated and has a dip of about 83°.

The roof of the coalbed, mainly made up of mudstone and sandy mudstone, has a variable thickness. Locally, the CP coal is in direct contact with its overlying sandstone. Both the thickness and lithology of the floor of the CP2 coal vary considerably as well, with a thickness from 0.2 to 2.0 m and a lithological composition of sandy sandstone, medium-coarse sandstone, and fine sandstone.

The lower portion of the Shuanmazhuang Formation is mainly made up of granule conglomerate, conglomerate, siltstone, sandy mudstone, and intercalated thin coalbeds.

The Permian strata, overlying the Shuanmazhuang Formation, include the Zahuaigou and Shiyewan Formations (Fig. 2). The upper portion of the Zahuaigou Formation is composed of mudstone and sandstone, and the lower portion is made up of white quartz-pebble conglomerate and locally intercalated 0.1–0.2 m mudstone beds. There are no minable coal beds in the Zahuaigou Formation. The Shiyewan Formation consists mainly of thick layers of sandstone, interbedded with mudstone.

The Cambrian–Ordovician strata underlying the coal-bearing sequences are dominated by limestone and are intercalated with silty mudstone in the lower portion.

The zoned distribution of the coal rank in the coalfield (Fig. 1B) is entirely related to igneous intrusions, which were associated with the Yanshan Movement of the Late Jurassic and Early Cretaceous Epochs (Zhong and Chen, 1988). In the east of the coalfield, igneous rocks have invaded into the coal-bearing strata (Fig. 2). The coal rank increases from the northwest to the southeast, from high volatile bituminous (hvb), through medium volatile bituminous (mvb), to low volatile bituminous (lvb) (Fig. 1B).

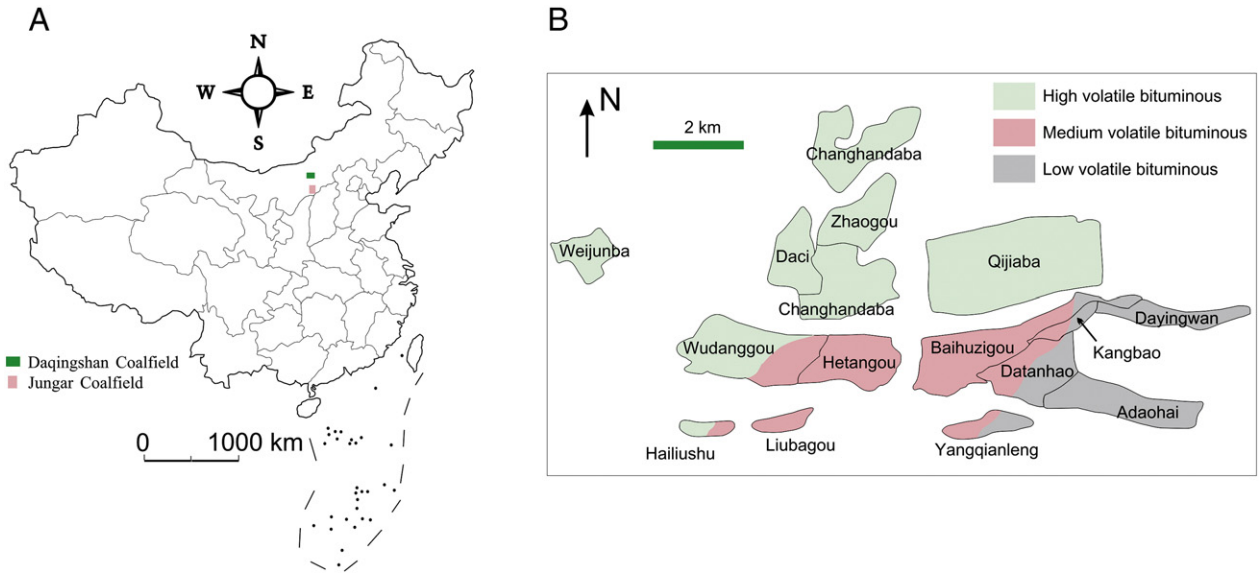

Fig. 1. Location of the Daqingshan Coalfield (A) and coal-rank distribution in the different mines of the coalfield (B).

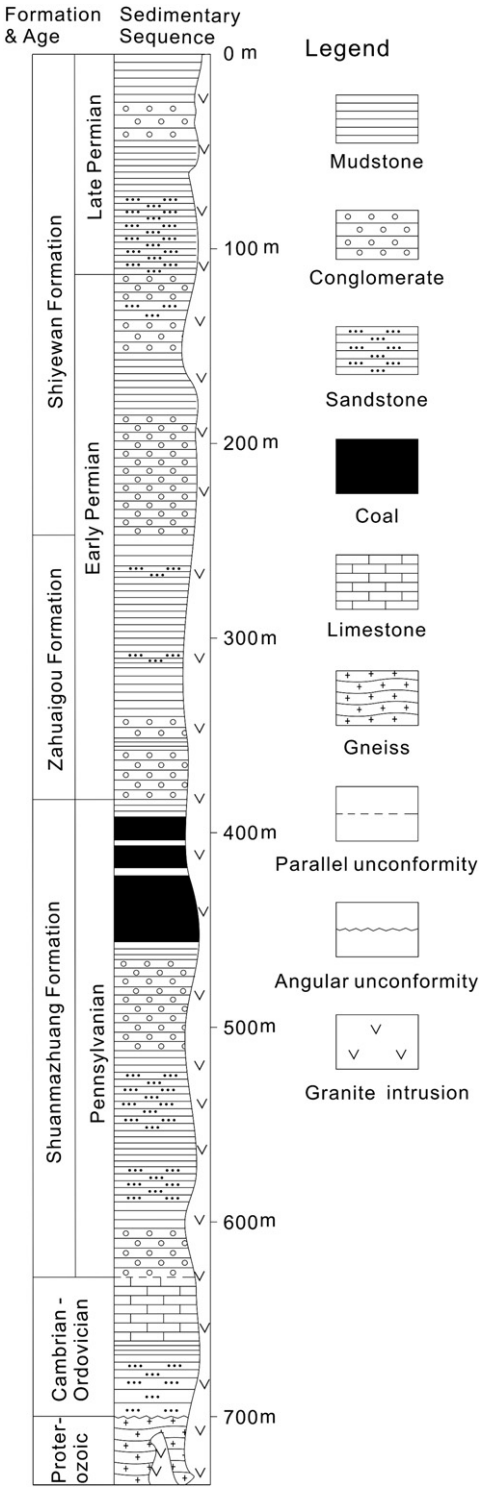

Fig. 2. Sedimentary sequences of the Daqingshan Coalfield.

3. Samples and analytical procedures

A total of 48 bench samples were taken from the face of the mined coal at the Adaohai Mine, Daqingshan Coalfield, following the Chinese Standard Method GB482-1985; these include 33 coal benches, 11 partings, and four roof samples (Fig. 3). Each coal bench sample was cut over an area 10-cm wide, 10-cm deep, and 50-cm thick. All collected samples were immediately stored in plastic bags to minimize contamination and oxidation. Sample number, thickness, and lithology data are shown in Fig. 3. From bottom to top, the 33 bench samples and the 11 partings (with a suffix -P) are identified as A1 to A44. The roof samples from bottom to top are Roof-1 to Roof-4. The cumulative thickness of the CP2 coal at this section is 36.37 m, of which partings amount to 22.85%.

Proximate analysis was conducted using ASTM Standards D3173-03, D3175-02, and D3174-04. The total sulfur and forms of sulfur were determined following ASTM Standards D3177-02 and D2492-02, respectively. Samples were prepared for microscopic analysis in reflected light following ASTM Standard D2797-04. Mean random reflectance of vitrinite (percent $R_{o,ran}$) was determined according to ASTM D2798-05, using a Leica DM4500P microscope (at a magnification of 500×) equipped with a Craic QDI 302™ spectrophotometer. Although ASTM D2798-05 requires a photomultiplier tube and a photometer amplifier for vitrinite reflectance determination, the Craic QDI spectrophotometer offers a charge-coupled detector (CCD) and thermoelectric cooling for improved spectral performance. The standard reference for vitrinite reflectance determination was gadolinium gallium garnet (Chinese Standard Reference GB13401) with a calculated standard reflectance 1.72% in oil at 546 nm.

The mineralogy was determined by optical microscopic observation and powder X-ray diffraction (XRD). Low-temperature ashing of coal was performed on an EMITECH K1050X Plasma Asher. XRD analysis of the low-temperature ashes and the parting samples was performed on a D/max-2500/PC powder diffractometer with Ni-filtered Cu–Kα radiation and a scintillation detector. The XRD pattern was recorded over a 2θ interval of 2.6–70°, with a step size of 0.01°. X-ray diffractograms of 48 samples (partings, roof, and coal LTAs) were subjected to quantitative mineralogical analysis using Siroquant™, commercial interpretation software developed by Taylor (1991) based on the principles for diffractogram profiling set out by Rietveld (1969). Further details indicating the use of this technique for coal-related materials are given by Ward et al. (1999, 2001) and Ruan and Ward (2002).

A scanning electron microscope (Hitachi S-3400N, 20 kV accelerating voltage) in conjunction with an energy-dispersive X-ray spectrometer (SEM-EDX) was used to study the characteristics of the minerals, and also to determine the distribution of some elements in the coal.

Samples were crushed and ground to pass 200 mesh for geochemical analysis. An elemental analyzer (vario MACRO) was used to determine the percentages of C, H, and N in the coal. X-ray fluorescence spectrometry (ARL ADVANT'XP+) was used to determine the oxides of major elements for the coal ash (815 °C), including SiO_2, Al_2O_3, CaO, K_2O, Na_2O, Fe_2O_3, MnO, MgO, TiO_2, and P_2O_5, and arsenic as well. Inductively coupled plasma mass spectrometry (X series II ICP-MS), in a pulse counting mode (three points per peak), was used to determine trace elements in the coal samples, except for Hg, F, and Cl. Mercury was determined using a Milestone DMA-80 Hg analyzer. Fluorine and Cl were determined by pyrohydrolysis with an ion-selective electrode, following the methods described in Chinese Standards GB/T 4633–1997 and GB/T 3558–1996.

4. Results and discussion

4.1. Coal chemistry and vitrinite reflectance

Table 1 summarizes the proximate and ultimate analyses, forms of sulfur, and random vitrinite reflectance data for the 33 coal benches from the Adaohai Mine. The average vitrinite reflectance and average volatile matter (daf) are 1.58% and 21.65%, respectively, indicating a low volatile bituminous coal (lvb) according to the ASTM classification (ASTM D 388–99).

The CP2 coal is a medium-ash and low-sulfur coal, according to Chinese Standards GB 15224.1-2004 (coals with ash yield 16.01%–29% are medium-ash coal) and GB/T 15224.2-2004 (coals with total sulfur content <1% are low-sulfur coal), with the exception of A7, A23, A24, and A44 which have 1.01–1.09% $S_{t,d}$. The sulfur is mainly organic (Table 1).

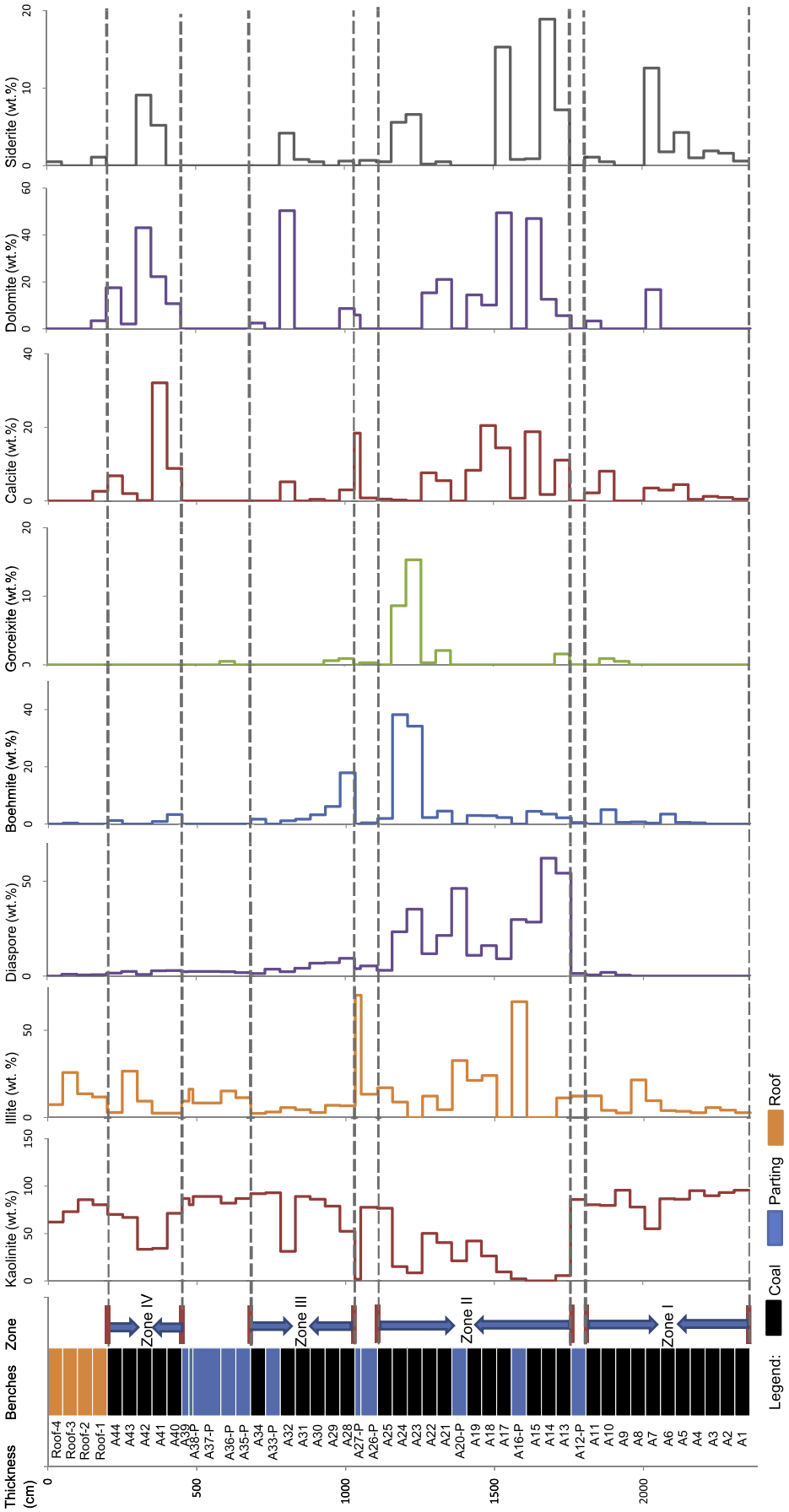

Fig. 3. Vertical variations of minerals in the coal.

Table 1
Proximate and ultimate analyses, forms of sulfur, and random vitrinite reflectance of the CP2 coal in the Adaohai Mine (%).

Sample	Proximate analysis			Ultimate analysis				Forms of sulfur			$R_{o,ran}$
	M_{ad}	A_d	V_{daf}	C_{daf}	H_{daf}	N_{daf}	$S_{t,d}$	$S_{p,d}$	$S_{s,d}$	$S_{o,d}$	
A44	0.28	14.17	19.37	89.62	4.47	1.41	1.09	bdl	0.02	1.07	1.57
A43	0.45	34.16	22.84	87.03	4.85	1.01	0.71	nd	nd	nd	1.55
A42	0.42	18.97	18.98	88.49	3.92	1.36	0.79	nd	nd	nd	1.61
A41	0.45	23.26	23.28	85.56	4.05	1.15	0.71	nd	nd	nd	1.59
A40	0.19	23.57	21.74	87.88	4.34	1.31	0.90	nd	nd	nd	1.66
A34	0.61	38.60	23.79	84.47	4.50	0.90	0.54	nd	nd	nd	1.62
A32	0.48	32.84	27.99	81.10	3.73	1.26	0.58	nd	nd	nd	1.61
A31	0.58	46.48	26.99	84.06	5.11	0.97	0.47	nd	nd	nd	1.59
A30	0.49	36.85	23.47	83.88	4.67	1.52	0.62	nd	nd	nd	1.63
A29	0.53	23.28	19.18	87.27	4.39	1.67	0.85	nd	nd	nd	1.63
A28	0.51	22.58	21.08	88.08	4.53	1.30	0.91	nd	nd	nd	1.46
A25	0.64	34.70	22.10	85.57	4.68	1.08	0.71	nd	nd	nd	1.61
A24	0.51	15.55	19.09	89.86	4.54	1.68	1.01	bdl	0.02	0.99	1.55
A23	0.06	12.26	18.86	89.5	4.54	1.37	1.08	bdl	0.01	1.07	1.59
A22	0.24	25.33	22.62	87.55	4.47	1.13	0.86	nd	nd	nd	1.57
A21	0.11	20.00	22.25	88.45	4.37	1.55	0.91	nd	nd	nd	1.54
A19	0.22	18.44	20.95	88.37	4.41	1.36	0.94	nd	nd	nd	1.66
A18	0.31	22.59	19.74	88.59	4.44	1.34	0.67	nd	nd	nd	1.49
A17	0.27	19.98	24.21	85.83	3.92	1.24	0.82	nd	nd	nd	1.61
A15	0.43	12.58	16.40	90.29	4.02	1.42	0.84	nd	nd	nd	1.56
A14	0.31	5.37	16.40	91.50	4.26	1.49	0.93	nd	nd	nd	1.62
A13	0.26	5.24	16.26	91.34	4.23	1.48	0.98	nd	nd	nd	1.60
A11	0.43	38.25	23.63	81.83	5.22	0.91	0.56	nd	nd	nd	1.57
A10	0.15	12.55	18.29	89.50	1.40	6.74	0.86	nd	nd	nd	1.53
A9	0.52	39.05	23.44	84.18	5.24	0.85	0.53	nd	nd	nd	1.56
A8	0.35	35.63	22.65	83.33	5.15	1.69	0.58	nd	nd	nd	1.47
A7	0.34	45.22	38.03	76.76	4.62	1.13	1.08	0.60	bdl	0.48	1.57
A6	0.26	11.17	17.18	89.83	4.66	2.25	0.86	nd	nd	nd	1.63
A5	0.34	21.89	19.57	88.48	4.80	1.15	0.72	nd	nd	nd	1.53
A4	0.36	23.49	19.74	87.58	4.88	1.27	0.70	nd	nd	nd	1.55
A3	0.44	24.55	19.58	87.84	4.76	1.27	0.67	nd	nd	nd	1.60
A2	0.50	33.07	22.07	85.37	4.97	1.17	0.58	nd	nd	nd	1.69
A1	0.46	33.45	22.75	84.93	5.16	1.39	0.67	nd	nd	nd	1.50
Av.	0.38	25.10	21.65	86.79	4.46	1.48	0.78	nd	nd	nd	1.58

M, moisture; A, ash yield; V, volatile matter; C, carbon; H, hydrogen; N, nitrogen; S_t, total sulfur; S_p, pyritic sulfur; S_o, organic sulfur; ad, air-dry basis; d, dry basis; daf, dry and ash-free basis; $R_{o,ran}$, random reflectance of vitrinite; av., average; nd, not detected; bdl, below detection limit.

Compared to the coals from the Heidaigou ($A_d = 17.72\%$, $S_{t,d} = 0.73\%$; Dai et al., 2006) and Haerwusu ($A_d = 18.34\%$, $S_{t,d} = 0.46\%$; Dai et al., 2008) surface mines in the Jungar Coalfield, the Adaohai coals from the Daqingshan Coalfield have a slightly higher ash yield and similar sulfur content. The rank of the coal, however, is much higher than that of coals from the Jungar Coalfield reported by Dai et al. (2006, 2008).

4.2. Maceral content of the CP2 coal

Table 2 lists the maceral contents of the CP2 coal. Inertinite is enriched in the coal (13.8–71.2%; 35.3% on average), compared to the late Paleozoic coals in northern China (generally less than 25%; Han, et al., 1996), but is much lower than that in the Jungar Coalfield (46.1–52.9%, mineral-free basis; Dai et al., 2006, 2008). The inertinite is dominated by semifusinite (12.5% on average), followed by macrinite (8.7% on average) and fusinite (6.3% on average).

The vitrinite is mainly composed of collodetrinite (28.9% on average) and telinite (3.3–50.2%, 27.5% on average), followed by collotelinite (6.9% on average).

4.3. Minerals found in the CP2 coal and their vertical variations

The proportion of each crystalline phase identified from the diffractograms of the coal LTAs, partings, and roof samples is given in Table 3. The phases identified in the samples include kaolinite, illite, diaspore, and boehmite, along with calcite, dolomite (or ankerite), siderite and, in some samples, quartz, pyrite, anatase, an aluminophosphate mineral of the gorceixite group, and trace amounts of fluorapatite and anatase.

Based on considerable vertical variations in the mineral proportions, the PC2 coal can be divided vertically into four zones: Zone I (from the lowest bench A1 to A11), Zone II (A13 to A25), Zone III (A28 to A34), and Zone IV (A40 to A44).

4.3.1. Kaolinite

The XRD pattern shows that the kaolinite in the coal LTAs, the roof, and the partings (Fig. 4) has a well-ordered structure. Kaolinite in the coal occurs as cell-fillings in telinite and fusinite. This is common in many other coals and closely associated strata, and may indicate formation by authigenic processes (Ward, 1989). The proportion of kaolinite is much lower in Zone II (averages 25.1%) than in Zones I (averages 85%), III (averages 71.6%), and IV (averages 55.2%) (Fig. 3).

In addition to the oxidized bauxite in the weathered crust of the Benxi Formation, as described below, it is believed that the sediment source region during peat accumulation was the Middle Proterozoic moyite of the Yinshan Oldland to the N and W of the coalfield (Wang, 1996). Consequently, clay minerals of terrigenous origin are important components in the coal seam, comparable to those in the wide area of the North China Coal Basin (Dai et al., 2006).

4.3.2. Illite

The illite in the samples typically has the XRD characteristics of an ammonian illite, with a slightly higher d(001) crystallographic spacing relative to more common K-bearing illites and other XRD peaks consistent with the ammonian illite (or tobelite) structure (Fig. 4). As discussed further by Daniels and Altaner (1990, 1993), Ward and Christie (1994), and Nieto (2002), the presence of ammonian illite may reflect the decomposition of organic nitrogen in the coal during rank advance or hydrothermal alteration, and

Table 2
Maceral contents determined under optical microscope for coals from the Adaohai Mine (vol.%; on mineral-free basis).

Sample	T	CT	CD	CG	VD	TV	SF	F	Mac	Mic	Fg	ID	TI
A44	31.8	18.9	33.1	bdl	bdl	83.8	6.2	3.6	4.1	0.2	bdl	2.1	16.2
A43	36.9	5.2	33.2	0.3	1.8	77.4	12.9	1.8	5.8	0.5	bdl	1.6	22.6
A42	30.0	1.0	20.2	bdl	bdl	51.2	24.7	7.2	6.0	bdl	bdl	10.9	48.8
A41	50.2	9.0	22.7	2.7	1.5	86.1	5.2	1.6	4.1	bdl	0.2	2.7	13.8
A40	3.3	30.1	30.7	0.3	14.1	78.5	11.3	1.2	1.1	bdl	bdl	7.8	21.4
A34	13.9	0.3	14.4	bdl	0.3	28.9	10.7	16.8	26.5	bdl	bdl	17.2	71.2
A32	27.5	11.5	27.9	bdl	8.7	75.6	9.4	5.0	4.3	0.2	bdl	5.4	24.3
A31	14.9	6.1	28.4	0.3	0.7	50.4	21.9	5.0	10.1	bdl	bdl	12.6	49.6
A30	21.3	2.5	35.7	bdl	bdl	59.5	8.9	5.4	17.5	bdl	bdl	8.7	40.5
A29	29.7	5.7	37.6	bdl	0.2	73.2	10.1	2.6	6.4	0.2	bdl	7.5	26.8
A28	28.7	13.6	29.5	bdl	bdl	71.8	10.1	3.5	10.2	0.9	bdl	3.5	28.2
A25	30.6	5.2	33.7	bdl	1.0	70.5	11.8	4.4	8.0	bdl	bdl	5.2	29.4
A24	38.5	3.6	37.2	bdl	bdl	79.3	7.3	3.0	4.7	0.3	bdl	5.5	20.8
A23	49.8	6.8	22.7	bdl	0.2	79.5	7.2	8.0	2.0	bdl	bdl	3.3	20.5
A22	41.7	4.9	28.9	0.7	1.0	77.2	7.2	3.9	6.5	0.2	bdl	4.9	22.7
A21	34.5	1.4	41.1	0.2	1.3	78.5	8.8	3.4	5.0	0.2	bdl	4.0	21.4
A19	33.9	6.1	31.3	bdl	bdl	71.3	6.1	6.3	8.7	bdl	bdl	7.6	28.7
A18	23.6	8.2	27.9	0.3	1.7	61.7	12.5	10.7	9.9	bdl	bdl	5.1	38.2
A17	24.5	11.5	22.4	0.8	0.5	59.7	19.0	9.7	6.6	bdl	bdl	4.9	40.2
A15	9.4	3.6	50.9	bdl	0.6	64.5	15.4	4.4	5.7	1.4	bdl	8.6	35.5
A14	28.7	6.2	34.6	bdl	bdl	69.5	6.7	3.5	7.3	bdl	bdl	13.0	30.5
A13	33.4	4.4	22.6	bdl	bdl	60.4	27.9	0.9	3.7	bdl	bdl	7.2	39.7
A11	13.6	4.3	36.8	bdl	bdl	54.7	11.7	0.3	19.3	0.5	bdl	13.4	45.2
A10	23.2	3.6	39.6	bdl	0.6	67.0	10.4	7.4	7.1	bdl	bdl	8.1	33
A9	37.3	1.8	12.8	bdl	2.6	54.5	16.4	9.1	7.3	bdl	bdl	12.8	45.6
A8	33.2	4.7	11.9	bdl	2.2	52.0	13.5	10.9	11.7	bdl	bdl	11.9	48.0
A7	25.1	4.6	29.3	bdl	1.2	60.2	12.3	7.1	14.2	bdl	0.3	5.8	39.7
A6	20.5	5.5	40.7	bdl	bdl	66.7	12.7	5.3	6.5	0.6	bdl	8.1	33.2
A5	24.5	7.9	16.6	0.3	0.8	50.1	15.7	7.1	15.4	bdl	bdl	11.7	49.9
A4	25.4	8.8	17.8	bdl	0.9	52.9	11.5	16.3	10.2	0.2	bdl	8.9	47.1
A3	11.6	2.3	41.7	0.3	1.0	56.9	15.1	10.2	8.1	bdl	bdl	9.7	43.1
A2	33.6	2.9	19.4	bdl	bdl	55.9	13.4	13.3	10.9	bdl	bdl	6.5	44.1
A1	21.3	14.8	20.1	bdl	bdl	56.2	19.9	8.8	12.1	bdl	bdl	3.0	43.8
av.	27.5	6.9	28.9	Trace	1.3	64.7	12.5	6.3	8.7	Trace	Trace	7.6	35.3

T, telinite; CT, collotelinite; CD, collodetrinite; CG, corpogelinite; VD, vitrodetrinite; TV, total vitrinites; SF, semifusinite; F, fusinite; Mac, macrinite; Mic, micrinite; Fg, funginite; ID, inertodetrinite; TI, total inertinites; av., average; Trace, trace content; bdl, below detection limit.

associated release of aqueous ammonium ions (NH_4^+) into the pore fluids. Interaction of the NH_4^+ with K-illite and/or kaolinite already present, either in the mineral matter of the coal or in the intra-seam partings, would then have resulted in the formation of ammonian illite by the incorporation of NH_4^+ instead of K^+ into the crystal structure (see Boudou et al., 2008; and references therein).

The ammonian illite is enriched in Zone II, where kaolinite makes up a lower proportion of the mineral matter than in Zones I, III, and IV (Fig. 3). The mode of occurrence of illite is similar to that of kaolinite; however, the ammonian illite in the coal may have been formed at a relatively high temperature by interaction of kaolinite with nitrogen released from the organic matter in coal during metamorphism caused by the igneous intrusion. The granite intrusions in the coalfield are attributed to the Yanshan Movement, one of the important tectonic events in China occurring in the Late Jurassic and Early Cretaceous Epochs. This is perhaps the reason why the proportions of kaolinite and ammonian illite vary inversely along the section. The minerals already present in the coal may have been affected and altered by the heat of the igneous intrusions. For example, Ward et al. (1989) reported the formation of illite from epiclastic or pyroclastic smectite in an Australian coal at the contact with an igneous intrusive body. Kwiecinska et al. (1992) described the development of illite close to an igneous dyke in a Polish coal seam. Burger et al. (1990) found that kaolinite and kaolinite-derived illite respectively occur in low- and high-rank coals and their corresponding intraseam tonsteins in eastern Yunnan, southwestern China.

4.3.3. Diaspore, boehmite, gorceixite, and fluorapatite

The mineral identified as gorceixite (Ba-aluminophosphate) in Table 3 has a structure between that of gorceixite, goyazite (Sr-aluminophosphate), and crandallite (Ca-aluminophosphate). It is thus probably an intermediate phase, representing a solid solution between these three end members (Ward et al., 1996). This is supported by SEM-EDX data (Table 4) and by comparisons with the chemical (trace element) analysis, as described below.

Diaspore, boehmite, and gorceixite make up a significant proportion of the minerals of samples A13 to A24 (Zone II in Fig. 3). However, diaspore and boehmite are also present as minor components of the mineral matter throughout most of the overlying Zone III (especially Sample A28), and to a lesser extent in Zones I and IV. Gorceixite is absent in Zone IV and in most benches of Zones I and III. Diaspore is also common in the partings (Table 3), but except for A26-P, boehmite and gorceixite are either absent or occur only in trace proportions (<0.5% of mineral matter) in the parting materials.

Diaspore (Fig. 5A, B) and boehmite generally occur as cell-fillings and in the collodetrinite or macrinite of the coal (Fig. 5C), and sometimes occur in distorted cells (Fig. 5D).

Gorceixite generally occurs in the cells of fusinite (Fig. 5A, B, D), semifusinite or telinite, and in collodetrinite (Fig. 6A). The relationship between diaspore and gorceixite indicates that the latter probably formed earlier than the former (Fig. 6A, B). Fluorapatite is very rare in the coal, only observed under SEM but below the detection limit of the XRD, and generally occurs as cell-fillings (Fig. 7). The modes of occurrence of diaspore, gorceixite, and fluorapatite indicate an authigenic origin.

Aluminum-hydroxide minerals, including boehmite and gibbsite, have been identified in some coals (Dai et al., 2006, 2008, 2010; Kalaitzidis et al., 2010; Wang et al., 2011a,b; Ward, 2002). The high proportion of boehmite in the coals from the Jungar Coalfield may have been derived from the exposed bauxite of the Benxi Formation in the sediment source region. Colloidal solutions of gibbsite may have been transported from the weathered crustal surface to the peat mire.

Table 3
Mineral compositions of parting and LTA samples of coal by XRD analysis and Siroquant (%; on organic matter-free basis).

Sample	LTA yield	Quartz	Kaolinite	Illite	Diaspore	Boehmite	Calcite	Dolomite	Siderite	Gorceixite	Anatase	Pyrite
Roof-4	nd	30.0	62.1	7.4					0.5			
Roof-3	nd		73.0	25.7	1.0	0.3						
Roof-2	nd		85.7	13.6	0.6							
Roof-1	nd		80.4	11.7	0.7		2.6	3.4	1.1			
A44	21.68		70.2	2.8	1.6	1.2	6.8	17.5				
A43	nd		66.9	26.5	2.4		2.0	2.1				
A42	nd		33.4	9.3	0.9		0.1	43.1	9.1		4.1	
A41	35.56		34.4	2.4	2.8	0.9	32.1	22.2	5.2			
A40	30.52		71.3	2.5	2.9	3.3	8.8	10.7			0.6	
A39-P	nd	0.5	87.0	9.4	2.3						0.9	
A38-P	nd		80.4	16.2	2.4						1.0	
A37-P	nd		89.2	8.3	2.5							
A36-P	nd		82.1	15.1	2.3					0.5		
A35-P	nd		87.0	11.3	1.8							
A34	45.49		92.0	2.3	1.4	1.7		2.5				
A33-P	nd	0.5	92.9	3.1	3.6							
A32	45.72		31.2	5.6	2.3	1.1	5.2	50.4	4.2			
A31	53.40		89.0	4.5	4.1	1.7			0.8			
A30	43.18		86.3	2.8	6.8	3.2	0.4		0.5			
A29	27.91		78.8	6.9	7.1	6.1				0.6	0.5	
A28	27.29		52.3	6.7	9.4	17.9	3.0	8.7	0.6	0.9	0.4	
A27-P	nd	0.2	1.7	70.0	3.9		18.4	5.9				
A26-P	nd	0.3	77.7	13.3	5.4	0.4	0.8		0.7	0.3	1.1	
A25	40.99		76.8	17.0	3.0	1.9	0.5		0.5		0.3	
A24	nd		15.2	8.8	23.4	38.2	0.2		5.6	8.6		
A23	15.01		8.6		35.3	34.2			6.6	15.3		
A22	30.02		50.1	12.3	11.8	2.3	7.6	15.3	0.2	0.3		
A21	23.82		40.4	4.5	21.4	4.5	5.5	21.0	0.5	2.1		
A20-P	nd		21.1	32.6	46.3							
A19	22.37		42.1	21.3	10.9	3.0	8.3	14.5				
A18	26.72		26.4	24.0	16.1	2.9	20.5	10.1				
A17	nd		9.5		9.1	2.3	14.4	49.5	15.3			
A16-P	nd		2.1	66.3	29.8		0.7		0.8		0.3	
A15	nd				28.5	4.4	18.8	47.0	0.9		0.5	
A14	6.13				62.2	3.5	1.7	12.6	18.9		1.1	
A13	6.44		5.5	11.2	54.3	2.2	11.1	5.6	7.2	1.6	1.3	
A12-P	nd		85.9	12.2	1.4	0.5						
A11	68.41		80.4	12.4	0.6		2.2	3.3	1.1			
A10	15.01	0.3	79.5	4.0	1.9	5.0	8.1		0.5	0.9		
A9	45.95	0.2	95.6	2.6	0.5	0.6				0.5		
A8	40.81		77.8	21.5		0.7						
A7	nd		55.0	9.6		0.3	3.5	16.7	12.6			2.3
A6	12.37		86.6	3.9		3.5	2.9		1.8		1.3	
A5	25.52		86.3	3.5		0.6	4.4		4.3		0.9	
A4	27.58		95.2	2.7		0.4	0.4		1.0		0.4	
A3	nd	0.2	89.9	5.6			1.2		1.9		1.2	
A2	39.00		93.3	4.2			0.9		1.6			
A1	39.51		95.7	2.7			0.5		0.6		0.5	

nd, no data.

Because of the compaction of the overlying strata after peat accumulation, the gibbsite colloid in the coal benches had begun to dehydrate, leading to boehmite formation (Dai et al., 2006, 2008).

Although some of diaspore occurs as isolated and discrete particles in macrinite and collodetrinite (Figs. 5C, 7A), the cell-filling modes of occurrence of diaspore (Fig. 5A,B) indicate that it was not derived from detrital materials of terrigenous origin but deposited from solutions or colloids. A critical factor, however, is the absence of silica in the system, which if available would have formed kaolinite.

During the stage of the peat accumulation for Zone II, the sediment-source region N and E of the Daqingshan Coalfield was uplifted, leading to exposure of the bauxite in the Pennsylvanian Benxi Formation. The Daqingshan Coalfield was in the low-lying area between the Yinshan Oldland to the N and W and the upwarped Benxi Formation to the N and E. The terrigenous materials were derived not only from the Yinshan Oldland, but also from the bauxite of the Benxi Formation, resulting in a high proportion of gibbsite in addition to the clay minerals. The Al-rich solutions, derived from the bauxite on the weathered surface in the sediment-source region, were transported into the peat mire and then were precipitated as gibbsite after peat accumulation and during diagenesis.

The high temperature of the igneous intrusion caused by the Yanshan Movement not only produced the relatively high rank of coals in the Adaohai Mine, but also led to gibbsite dehydration and then to diaspore formation. However, the coals in the adjacent mines of the same coalfield (Fig. 1B), which were less subjected to the igneous intrusions, have a relatively low high-volatile-bituminous rank.

Gorceixite and fluorapatite may also have been derived from the bauxite on the weathered surface (Benxi Formation) in the sediment-source region, and deposited in the same period as the gibbsite formation but much earlier than the diaspore formation. Possibly P released from the organic matter in the peat was picked up by those Al-rich solutions to form essentially insoluble aluminophosphates in the pores of the organic matter. Dai et al. (2006) found goyazite in the middle portion of the No. 6 Coal of the Jungar Coalfield, which coexisted with boehmite.

However, trace amounts of Al-hydroxide- and gorceixite-forming materials were also derived from the upwarped Benxi Formation to

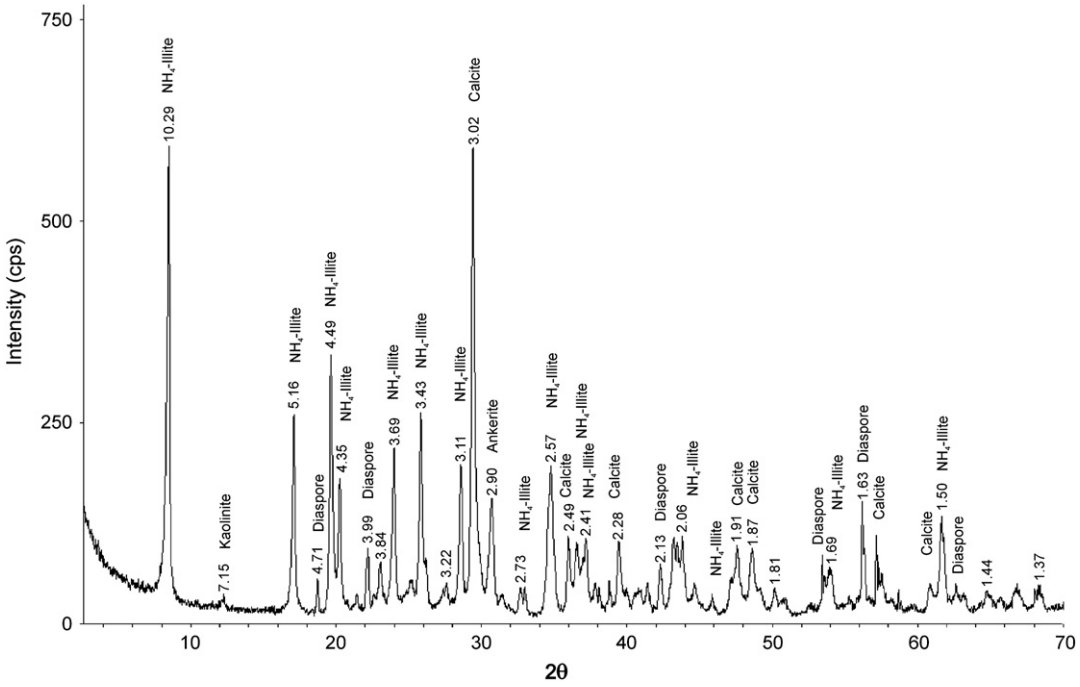

Fig. 4. X-ray diffractogram of sample A27-P, showing ammonian illite and other phases present.

the N and E during other periods of peat accumulation, corresponding to the lower and upper portions of the coal bed corresponding to Zones I, III, and IV, leading to minor amounts of diaspore, boehmite, and gorceixite in some benches. This indicates that the supply of terrigenous bauxitic materials from the upwarped Benxi Formation had become weak during the peat accumulation phases corresponding to Zones I, III, and IV.

The reason that the boehmite but not diaspore occurs in the Jungar coals is the relatively low-rank of the coal, which had not been subjected to high temperatures from igneous intrusions. The formation of diaspore requires a higher temperature than boehmite (Liang et al., 1997; Zhang, 1984).

4.3.4. Carbonate minerals

Carbonate minerals identified in the coal include calcite, dolomite, and siderite. The material identified as dolomite in Table 3 has an XRD pattern intermediate between that of dolomite and ankerite. It is thus probably an iron-bearing dolomite mineral. This is further supported by SEM-EDX data (Table 4) and the comparison of the XRD results with the chemical analysis as described below.

These carbonate minerals are abundant in Zone II and occur to a lesser extent in Zones I, III, and IV. Calcite and dolomite occur as cell- or fracture-fillings (Fig. 8A, B, C), indicating an epigenetic origin. The modes of occurrence of siderite (Fig. 8D) indicate that it has an epigenetic origin as well.

Carbonate minerals are common in coal and are formed during the complete range of its petrogenesis from the authigenic to epigenetic and post-coalification stages (Kortenski, 1992). However, carbonate minerals are less common in actual coal-forming environments, since the normally acidic peat-swamp waters are thought to preclude carbonate precipitation (Belkin et al., 2010; Bouška, et al., 2000; Dai and Chou, 2007). It has been reported that carbonate minerals are often abundant in the coal around igneous intrusions, introduced as epigenetic minerals mainly from hydrothermal alteration of the igneous material (Dai and Ren, 2007; Finkelman et al., 1998; Kisch and Taylor, 1966; Querol et al., 1997; Ward et al., 1989). It is generally believed that CO and CO_2 derived from carbonization of the coal interact with fluids derived from the magma to produce this carbonate mineralization (Ward, 2002). The other possible mechanism for carbonate mineralization in the coal is that, during rank

Table 4
SEM-EDX semi-quantitative analysis of some minerals in the coal (%; on carbon-free basis).

Mineral		O	F	Na	Mg	Al	Si	P	S	K	Ca	Sr	Fe	Zr	Mn	Ba
Fluorapatite (N = 2)	Min	35.37	3.41	0.01	0.02	0.01	0.01	19.09	bdl	bdl	35.85	bdl	0.01	2.31	bdl	0.01
	Max	33.95	4.82	0.02	0.07	0.03	0.15	19.12	bdl	bdl	36.74	bdl	0.09	2.96	bdl	0.03
	Av	34.66	4.11	0.01	0.04	0.02	0.08	19.11	bdl	bdl	36.3	bdl	0.05	2.63	bdl	0.15
Gorceixite (N = 14)	Min	33.79	bdl	bdl	bdl	11.66	bdl	9.18	bdl	bdl	0.09	bdl	bdl	bdl	bdl	10.76
	Max	60.64	4.71	0.13	0.74	19.58	bdl	18.27	1.98	0.16	4.11	7.43	bdl	3.85	bdl	43.53
	Av	47.78	1.21	0.04	0.09	14.72	bdl	12.07	0.62	0.03	1.71	4.01	bdl	1.67	bdl	16.19
Diaspore (N = 26	Min	53.89	bdl	bdl	bdl	20.62	bdl	bdl	bdl	bdl	bdl	bdl	bdl	0.01	bdl	bdl
	Max	76.97	bdl	0.34	0.14	46.11	1.07	6.65	1.38	0.3	1.07	1.24	bdl	0.99	bdl	5.52
	Av	58.77	bdl	bdl	bdl	38.62	0.09	0.78	0.08	0.02	0.09	0.06	bdl	0.11	bdl	0.54
Siderite (N = 4)	Min	52.31	bdl	bdl	4.7	bdl	bdl	bdl	bdl	bdl	0.14	bdl	32.76	bdl	bdl	bdl
	Max	57.1	bdl	0.06	9.91	0.04	bdl	bdl	bdl	bdl	2.95	bdl	41.28	bdl	1.13	bdl
	Av	53.65	bdl	bdl	6.71	bdl	bdl	bdl	bdl	bdl	1.27	bdl	38.1	bdl	0.38	bdl
Dolomite (N = 2)	Min	52.57	bdl	bdl	6.28	bdl	bdl	bdl	bdl	bdl	23.45	bdl	8.29	bdl	bdl	bdl
	Max	56.13	bdl	bdl	9.06	0.07	0.33	bdl	bdl	0.1	24.85	bdl	16.34	bdl	0.98	0.14
	Av	54.35	bdl	bdl	7.76	0.04	0.17	bdl	bdl	0.05	24.15	bdl	12.32	bdl	0.50	0.08
Clacite (N = 1)		52.41	bdl	bdl	bdl	bdl	bdl	bdl	bdl	bdl	47.16	bdl	bdl	bdl	bdl	bdl

N, number of test spots; Min, minimum; Max, maximum; Av, average; bdl, below detection limit (0.01%).

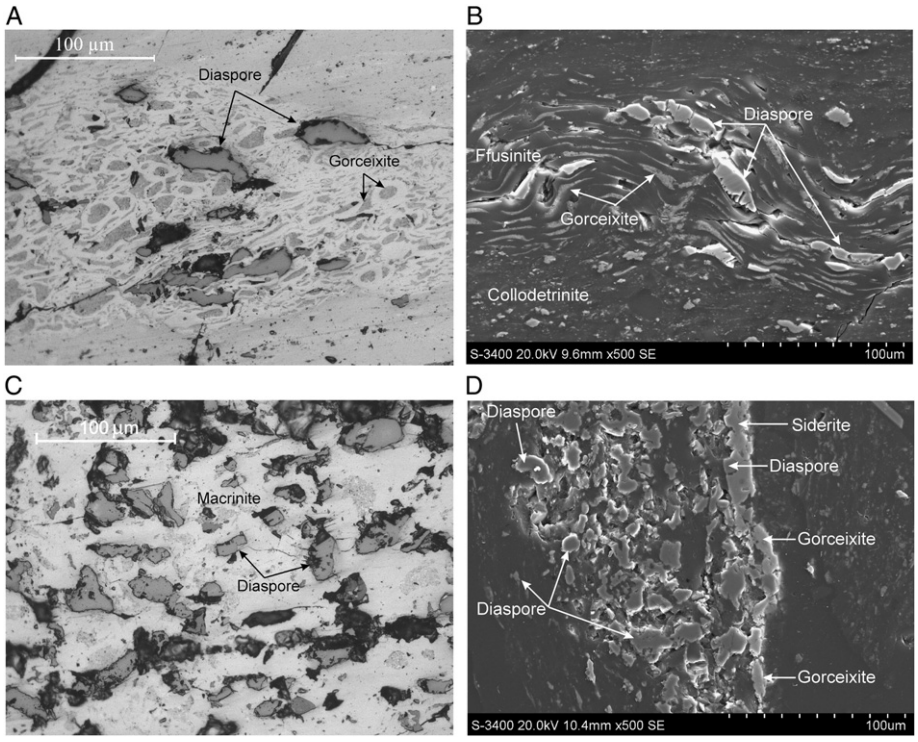

Fig. 5. Modes of occurrence of minerals in coal bench samples of Zone II. (A) and (B), Diaspore and gorceixite occurring in cells of fusinite; (C) Diaspore in macrinite; (D) Diaspore, gorceixite, and siderite in distorted cell and collodetrinite. Images A and C, reflected light; Images B and D, SEM and back-scattered electron images.

advance, Ca is released from the organic matter and migrates into and around the seam, interacting with CO_2 in the pore water and precipitating as fracture-fillings and similar deposits. The dolomite, calcite, and siderite in the Adaohai coals may have been derived from magmatic fluids during the Yanshan Movement of the Late Jurassic and Early Cretaceous Epochs. The carbonate mineral-enriched Zone II of the section is the portion where high illite and diaspore are also present, possibly reflecting the relatively high temperature of the fluids involved. However, the temperature of the fluids was not high enough to elevate the vitrinite reflectance (Table 1). It could also be that the carbonate forming fluids were the source of the high temperature for illite and diaspore formation, and that the carbonate minerals were in turn derived from the igneous intrusion.

4.3.5. Quartz, pyrite, and anatase

Quartz is only present in the uppermost roof sample (Roof-4, Table 3). Possible traces (0.2–0.5%) are indicated in several other samples, but if quartz is present at all in these samples its concentration is close to or below the detection limit of the XRD and Siroquant system.

Pyrite was only detected in bench A7 (2.3 wt.%). It occurs as fracture-fillings (Fig. 8A), indicating an epigenetic origin.

Trace proportions of anatase are present in all four zones, although it is absent or below detection limits in a number of coal and parting benches.

A similar mineralogical profile, with ammonian illite, diaspore, calcite, dolomite, and goyazite-gorceixite, as well as chlorite, has also been identified in the middle part of a relatively high-rank Permian coal seam in the South Walker Creek area of the northern Bowen Basin in Australia (Permana et al., 2010), suggesting that similar mineral-forming processes may occur in other areas and geological periods as well.

4.4. Elements in the coal

The abundances of major and trace elements in the coal benches, partings, and roof samples, in comparison to average values for

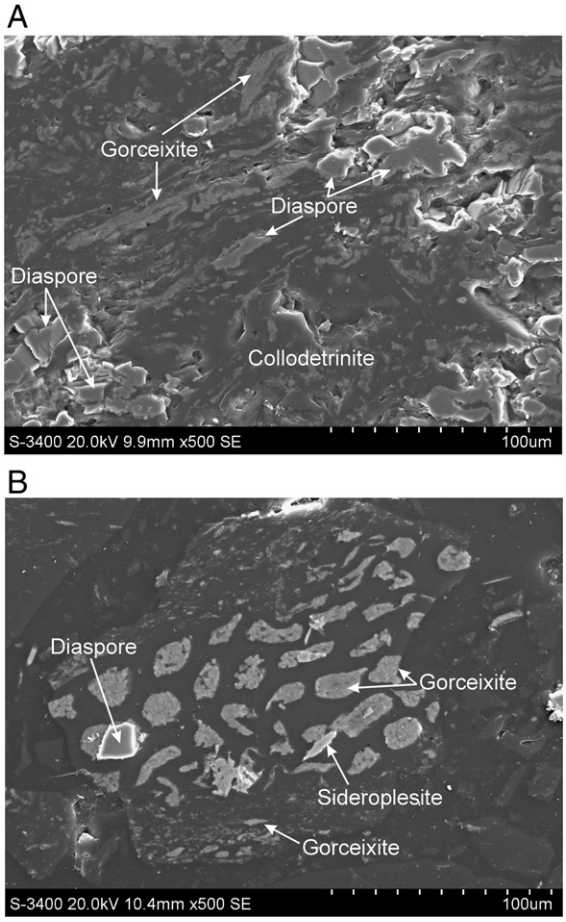

Fig. 6. Relation between gorceixite and diaspore in the coal. (A) Gorceixite in collodetrinite, diaspore in collodetrinite and distorted cells; (B) Gorceixite in coal-forming plant cells. Both A and B are SEM and back-scattered electron images.

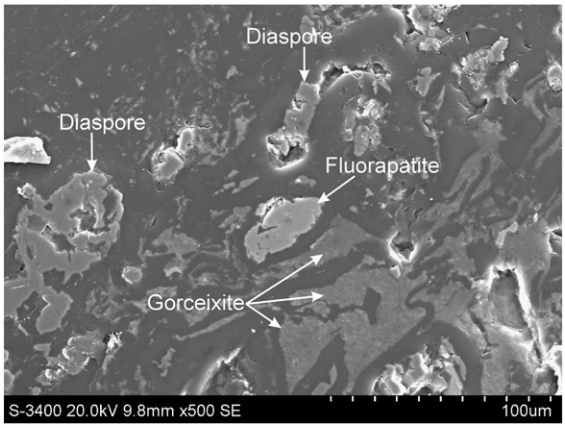

Fig. 7. Modes of occurrence of fluorapatite, gorceixite, and diaspore in the coal (SEM and back-scattered electron image).

Chinese and world coals, are listed in Table 5. Compared to those averages, the coals from Adaohai Mine have a lower SiO_2/Al_2O_3 ratio (0.93) and are higher in CaO (1.69%), MgO (0.32%), P_2O_5 (0.124%), F (207 μg/g), Ga (16.3 μg/g), Zr (446 μg/g), Ba (276 μg/g), Hg (0.33 μg/g), Pb (25.6 μg/g), and Th (12.4 μg/g).

4.4.1. Comparison between mineralogical and chemical compositions

The chemical composition of the (high-temperature) coal ash expected to be derived from the mineral assemblage indicated by the Siroquant analysis of each LTA or parting sample (Table 3) was calculated for a selection of samples (Table 6), using methodology described by Ward et al. (1999). This process includes calculations to allow for the loss of hydroxyl water from the clay and bauxite minerals and CO_2 from the carbonates, at the temperatures associated with high-temperature (815 °C) ashing and combustion processes.

Stoichiometric compositions were used for most of the minerals in the calculations. The composition of a normal K-bearing illite was used to represent the illite, and crandallite was taken to represent the gorceixite component. Following the indications of the XRD pattern as discussed above, the composition of an ankerite, with equal molecular proportions of Ca, Mg and Fe, was used to represent the dolomite component.

Chemical analysis data for the samples were recalculated to provide normalized percentages of the major element oxides in the inorganic fraction of each sample (Table 6). These are likely to represent the chemical composition of the (high-temperature) ash derived from each sample.

The percentages of SiO_2, Al_2O_3, K_2O, CaO, MgO, and Fe_2O_3 indicated by both sets of data (Table 6) were plotted against each other (Fig. 9), to provide a basis for comparing the XRD results to the chemical analysis data for the same coal or parting samples. As discussed for other materials by Ward et al. (1999, 2001), the respective data sets are presented as X–Y plots, with a diagonal line on each plot indicating where the points would fall if the estimates from the two different techniques were equal.

For SiO_2 and Al_2O_3, the points fall very close to the equality line, suggesting that the percentages of the various silicate minerals indicated by the XRD analysis are consistent with the independently-determined chemical data. Although a little more scattered, the plots

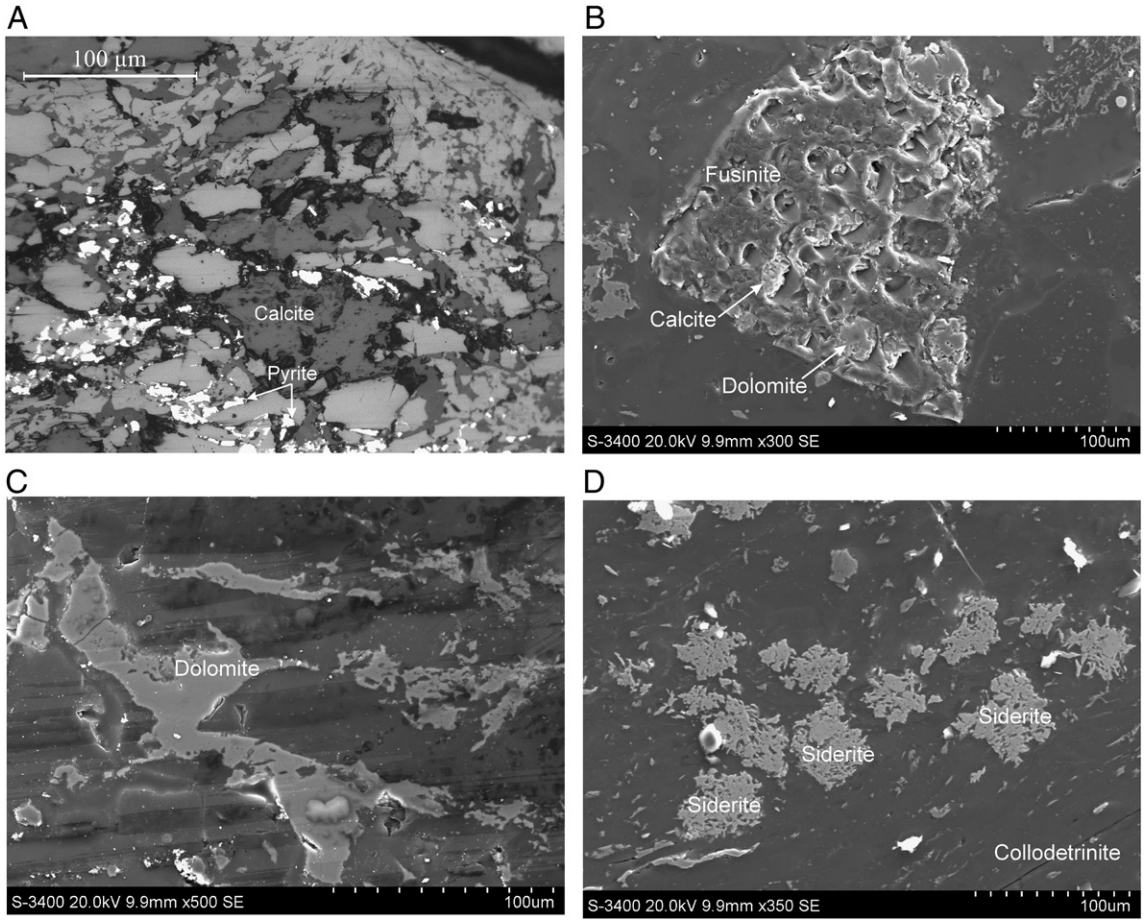

Fig. 8. Modes of occurrence of carbonate minerals and pyrite in the Adaohai coals. (A) Fracture-filling pyrite and calcite; (B) Cell-filling calcite and dolomite; (C) Fracture-filling dolomite; (D) Siderite in coal. Image A, reflected light; Images B–D, SEM and back-scattered electron images.

Table 5
Concentrations of major element oxides and trace elements in coal benches, partings, and roof samples from the Adaohai Mine (elements in μg/g, oxides in %; on whole-coal basis).

Sample	Al_2O_3	SiO_2	SiO_2/Al_2O_3	CaO	Fe_2O_3	K_2O	MgO	MnO	Na_2O	P_2O_5	TiO_2	Li	Be	F	Cl	Sc	V	Cr	Co	Ni	Cu	Zn	Ga	Ge
Roof-4	30.9	56.23	1.82	0.12	0.7	0.646	0.13	0.004	0.014	0.039	0.98	101	2.18	266	100	6.33	31.8	33.7	8.79	13.1	20.5	53.6	20.6	1.1
Roof-3	35.38	40.71	1.15	0.18	0.82	0.246	0.04	0.004	0.047	0.074	1.43	17.2	3.13	406	40	29.1	158	106	36.1	46.7	79.1	199	38.3	3.77
Roof-2	38.66	44.58	1.15	0.08	0.37	0.092	bdl	bdl	0.045	0.064	0.86	16.5	2.51	368	50	17	60.8	37.8	4.38	7.61	27.4	179	37.2	2.81
Roof-1	23.8	26.3	1.11	2.32	1.64	0.044	0.39	0.012	0.067	0.033	1.22	22.4	3.55	306	100	15.8	44.7	22.1	2.92	9.81	32.7	36.3	34.6	1.79
A44	6.04	5.97	0.99	1.22	0.36	0.007	0.14	0.003	0.022	0.017	0.35	4.6	1.05	91	150	7.73	62.7	15.2	10.6	7.71	16.5	16.7	12	0.99
A43	14.46	16.06	1.11	1.06	0.39	0.063	0.12	0.004	0.035	0.031	0.94	7.76	1.65	119	20	16.6	105	21.4	8.87	6.6	22.5	18.5	28.9	1.26
A42	4.49	4.3	0.96	3.92	2.84	0.026	1.21	0.028	0.017	0.029	1.81	2.81	2.48	141	150	27.9	75.2	26.1	3.75	9.92	35.1	21.8	14.4	2.28
A41	6.62	5.65	0.85	7.94	2.18	0.009	0.5	0.059	0.03	0.01	0.22	5.11	1.39	95.6	120	7.45	63.8	25.7	9.76	13.2	69.6	44.7	16.8	1.83
A40	9.77	9.63	0.99	1.79	0.62	0.019	0.17	0.008	0.036	0.031	0.53	5.82	2.15	124	100	9.46	60.4	21.7	10.6	17.3	68.4	96.2	19.1	1.83
A39-P	36.98	42.33	1.14	0.37	0.9	0.214	0.03	0.005	0.06	0.083	1.77	14	2.45	247	30	18.9	104	72	23.7	30.6	53.3	191	28.6	2.35
A38-P	32.47	37.22	1.15	0.56	1.27	0.284	0.11	0.009	0.052	0.081	1.25	17.4	1.8	240	140	21.2	266	116	28.2	36.9	62.3	139	31.2	2.2
A37-P	36.63	41.58	1.14	0.16	1.15	0.216	0.03	0.002	0.066	0.077	1.86	18.8	2.18	244	100	24.4	95.5	72.6	20	33.3	45.7	162	27.2	2.29
A36-P	37.02	42.26	1.14	0.13	1.33	0.336	0.06	0.01	0.067	0.092	1.34	19.3	2.68	270	bdl	21.8	132	88.2	19.3	33.4	78.5	136	36.8	3.25
A35-P	36.66	41.97	1.14	0.11	1.12	0.325	0.05	0.005	0.058	0.096	1.33	13.3	2.1	147	30	13.8	104	71.5	20.5	32	69.8	128	27.9	2.46
A34	17.19	18.67	1.09	0.57	0.68	0.034	0.12	0.006	0.054	0.074	0.87	9.46	3.09	128	bdl	20	64.8	30.6	2.31	7.92	54.5	32.1	25.3	2.41
A33-P	31.98	35.83	1.12	0.15	0.27	0.065	0.02	0.001	0.101	0.075	0.79	19.5	3.15	207	bdl	10.6	38.3	19.9	4.86	4.78	17.4	39.3	28.8	0.99
A32	7.93	7.1	0.9	8.38	4.73	0.024	2.46	0.054	0.025	0.055	0.48	5.01	1.93	124	bdl	18.1	81.1	28.7	3.73	9.27	33.2	25.3	24	2.86
A31	21.39	22.04	1.03	0.2	0.4	0.029	0.04	0.001	0.049	0.093	0.83	9.55	2.83	196	10	10.8	45	10.9	3.93	18.6	14.5	10.9	24.8	2.24
A30	17.4	18.2	1.05	0.21	0.29	0.017	0.03	0.002	0.04	0.056	0.68	8.73	2.52	117	60	12.3	54.2	18.6	5.96	10.5	19.9	20	22.4	1.56
A29	11.07	10.6	0.96	0.2	0.24	0.028	0.04	0.001	0.024	0.088	0.66	6.12	2.28	115	130	14.6	57.9	21.1	5.86	18.2	15.1	29.2	26.3	2.46
A28	12.49	6.01	0.48	1.04	0.58	0.046	0.16	0.006	0.026	0.302	0.57	5.19	1.92	248	290	9.52	41.4	18.7	8.57	20.6	21.4	26.6	15.2	1.05
A27-P	27.49	29.32	1.07	14.22	2.39	0.088	0.83	0.09	0.026	0.111	0.37	3.32	0.91	531	bdl	2.08	25.7	7.84	3.39	28.5	6.58	17.1	7.96	0.27
A26-P	24.95	26.99	1.08	0.55	0.35	0.086	0.04	0.001	0.071	0.059	1.18	17.8	1.75	393	bdl	10.4	41.3	14.7	2.41	10.3	13.8	23.6	12.3	0.54
A25	16.16	17.03	1.05	0.19	0.25	0.06	0.03	0.001	0.051	0.038	0.86	13.8	2.46	256	200	16.9	53.2	23.3	3.96	12.4	25.4	22.5	15.4	0.97
A24	10.69	2.41	0.23	0.39	0.29	0.039	0.04	0.004	0.016	1.023	0.44	3.08	2	824	380	7.83	30.6	15	8.13	10.5	17.5	44.6	16.2	1.76
A23	8.24	0.92	0.11	0.45	0.23	0.011	0.04	0.003	0.01	0.952	0.37	2.33	1.19	429	110	9.14	43.1	10.1	10.5	2.91	16.6	27	13.1	0.85
A22	10.6	9.08	0.86	2.53	0.7	0.024	0.41	0.008	0.037	0.169	0.41	9.06	1.45	151	110	8.76	45.2	16.2	6.58	6.51	16.4	23.1	13	0.88
A21	8.85	6.57	0.74	2.01	0.68	0.012	0.33	0.012	0.036	0.343	0.3	7.56	1.39	300	20	6.66	25.7	12.6	7.08	4.83	16.4	24	14.9	1.28
A20-P	39.25	27.05	0.69	0.52	0.46	0.189	0.09	0.005	0.044	0.37	0.92	12.1	2.07	1272	50	7.44	21.8	11.5	0.74	4.93	10.5	23.2	33.8	0.8
A19	8.79	7.48	0.85	1.42	0.41	0.016	0.2	0.005	0.034	0.03	0.22	9.48	0.89	165	bdl	2.99	15.8	11.1	3.6	3.7	10.4	20.9	6.65	0.53
A18	9.58	7.64	0.8	3.42	0.33	0.028	0.21	0.004	0.028	0.061	0.31	8.15	1.01	555	50	2.14	15.2	13.2	3.08	4.68	7.7	24.2	8.13	0.79
A17	4.38	2.01	0.46	6.49	4.13	0.005	1.45	0.103	0.026	0.028	0.1	3.04	0.87	204	100	2.32	12.4	12.6	3.02	6.68	7.54	13.2	6.09	0.55
A16-P	27.07	20.41	0.75	0.63	0.88	0.258	0.18	0.01	0.03	0.2	0.88	2.95	1.28	525	10	7.14	23.6	11.7	1.15	6.79	11.2	21	14.3	0.82
A15	4.54	0.1	0.02	3.95	1.18	0.001	0.91	0.023	0.005	0.107	0.1	bdl	1.18	199	bdl	2.78	11.7	7.3	1.85	2.43	8.1	15.7	5.67	0.52
A14	3.53	0.1	0.03	0.35	0.78	0.003	0.15	0.012	0.004	0.05	0.25	0.92	1.08	112	50	2.33	19.7	12.6	1.4	2.77	17.3	21.1	6.58	0.55
A13	3.28	0.72	0.22	0.41	0.29	0.005	0.05	0.004	0.01	0.077	0.14	2.08	0.91	153	bdl	1.27	15.2	12.1	2.04	3.72	9.93	76	6.45	0.79
A12-P	29.14	32.06	1.1	0.23	0.15	0.162	0.03	bdl	0.057	0.055	0.47	16.5	1.84	214	20	3.03	15.6	9.39	1.03	4.74	11.5	17.9	29.7	1.36
A11	17.65	18.73	1.06	0.3	0.14	0.075	0.05	bdl	0.037	0.133	0.82	11.5	2.58	371	120	5.78	28.5	13.4	1.36	2.51	15.1	37.9	19	1.24
A10	5.59	5.83	1.04	0.54	0.06	0.024	0.01	0.001	0.012	0.052	0.23	1.37	2.73	79.2	40	12.3	45.4	10.7	3.41	2.86	14.1	31.2	23.3	2.08
A9	18.01	20.22	1.12	0.1	0.09	0.046	0.01	bdl	0.043	0.138	0.45	7.73	2.89	270	160	9.22	28.6	13.5	1.3	4.07	10.6	23.5	29.1	3.78
A8	16.11	18.36	1.14	0.08	0.11	0.062	0.02	0.0004	0.028	0.03	0.55	5.01	2.28	114	bdl	6.79	23	9.94	2.23	1.48	12.1	12.7	14.9	0.99
A7	14.54	14.45	0.99	5.34	6.12	0.047	1.57	0.123	0.05	0.015	0.35	12.5	1.32	205	130	5.49	23.5	10.2	2.1	4.21	8.62	14.8	14.3	0.96
A6	4.81	5.27	1.1	0.23	0.16	0.01	0.02	0.002	0.008	0.004	0.53	4.06	2.09	87.6	140	11.3	39.4	14.9	3.49	3.89	92.2	28.1	13.2	1.68
A5	9.5	10.59	1.11	0.38	0.38	0.023	0.02	0.006	0.018	0.008	0.78	6.16	1.88	165	190	9.71	41.6	13.6	2.26	4.04	11.4	33	14.6	1.57
A4	10.51	11.91	1.13	0.11	0.24	0.021	0.02	0.004	0.018	0.009	0.58	5.99	1.6	132	bdl	5.99	33.6	10.2	2.01	3.5	9.12	8.14	10.3	0.63
A3	10.73	12.1	1.13	0.22	0.4	0.032	0.02	0.007	0.022	0.01	0.88	6.6	2.44	130	110	11.4	49.2	17.8	1.66	3.11	14.4	36.9	15.4	1.55
A2	14.88	16.84	1.13	0.19	0.38	0.026	0.01	0.006	0.034	0.016	0.6	15	2.26	201	70	11.3	64.5	16.7	2.13	4.2	18	23.1	16.2	1.27
A1	15	17	1.13	0.17	0.19	0.014	0.02	0.002	0.03	0.022	0.78	19	1.17	237	10	9.79	180	23.7	2.81	5.32	44.4	43.7	25.4	3.16
av.	10.75	9.99	0.93	1.69	0.94	0.027	0.32	0.016	0.028	0.124	0.55	7.02	1.85	207	116	9.6	47.2	16.3	4.54	7.28	23.5	28.7	16.3	1.49
China [a]	5.98	8.47	1.42	1.23	4.85	0.19	0.22	0.015	0.16	0.092	0.33	31.8	2.11	130	255	4.38	35.1	15.4	7.08	13.7	17.5	41.4	6.55	2.78
World [b]	nd	nd	nd	nd	nd	nd	nd	0.011	nd	0.053	0.133	12	1.6	88	180	3.9	25	16	5.1	13	16	23	5.8	2.2

av., average concentrations of elements in the CP2 coal; nd, not detected; bdl, below detection limit; [a], from Dai et al. (2011); [b], from Ketris and Yudovich (2009); [c], from Dai et al. (2008); nd, no data.

for CaO, MgO, and Fe_2O_3 are also relatively close to the equality line. The scatter is probably due in part to differences between the chemical composition used to represent dolomite (ankerite) in the calculation and the actual chemistry of the dolomite/ankerite in the samples themselves. In particular, the plots suggest that the dolomite may have more Ca and less Mg and Fe than that of the material used to calculate the inferred ash compositions.

The plot for K_2O, however, shows a considerable difference between the observed and inferred percentages. This is because the chemistry of a K-bearing illite was used in the calculation, whereas the illite in the samples is mainly an NH_4-bearing variety. The discrepancy between the two estimates is consistent with identification of the illite as an ammonian illite, which in turn explains the low proportion of K_2O found in chemical analysis despite the high proportion of illite indicated in the same samples by XRD.

4.4.2. Major elements in coal and vertical variations

The major element oxides in coals from the Adaohai Mine are dominated by Al_2O_3 and SiO_2 (Table 5), which are slightly higher respectively than those in the common Chinese coals reported by Dai et al. (2011). Because quartz is virtually absent (Table 3), the clay minerals are the major carrier of Si in the coal samples. In addition to a small proportion of Al in gorceixite, aluminum mainly occurs in the clay minerals and in the diaspore and boehmite.

As expected, the SiO_2/Al_2O_3 ratio for each bench of the CP2 coal (0.84 on average) is lower than the same ratio for kaolinite (1.18) and also lower than common values in Chinese coals (1.42; Dai et al., 2011). The SiO_2/Al_2O_3 ratios in the partings and in the lower part of Zone I are close to the ratio expected for pure kaolinite (1.18), but most of the other coals have slightly lower SiO_2/Al_2O_3 values. The SiO_2/Al_2O_3 ratio in coals from other areas is generally higher than that

As	Se	Rb	Sr	Y	Zr	Nb	Mo	Cd	In	Sn	Sb	Te	Cs	Ba	Hf	Ta	W	Re	Hg	Tl	Pb	Bi	Th	U
nd	0.11	25	25.3	10.8	282	17.2	0.8	0.15	0.07	4.65	0.13	0.05	1.61	186	11.3	1.08	5.77	bdl	0.11	0.45	17.8	0.18	11.7	2.43
nd	0.4	14	78.4	27.7	349	23.2	3.37	0.4	0.12	5.09	0.19	0.05	0.94	250	12.1	1.42	2.36	bdl	0.34	0.46	35.6	0.46	18.5	3.09
nd	0.28	4.59	31.8	18	382	28.7	1.7	0.54	0.08	4.82	0.12	0.06	0.35	192	14.2	2.2	1.57	bdl	0.63	0.3	49.9	0.34	31.3	5.3
nd	0.52	3.08	40	39.7	734	32.2	4.32	0.36	0.2	9.09	0.48	0.11	0.26	160	14.6	2.3	1.55	0.004	0.61	0.37	36.1	1.54	26.1	5.65
1	0.2	0.88	26.4	13.4	979	12.9	5.12	0.18	0.08	3.54	0.29	0.04	0.03	148	8.23	0.66	1	bdl	0.19	0.12	18.4	0.49	8.94	2.44
0.4	0.31	3.58	20.8	24.6	162	16.9	7.2	0.19	0.11	4.93	0.37	0.05	0.26	116	21.9	1.16	0.97	bdl	0.38	0.5	31.1	0.54	24.8	5.2
4.5	0.59	2.53	25.6	48.6	290	28.4	3.57	0.22	0.19	6.01	0.28	0.08	0.1	121	20.6	1.99	2.05	0.005	0.55	0.14	66.6	1.54	40.6	6.77
0.6	0.37	1.12	63.9	29.6	286	3.8	7.26	0.5	0.06	4.4	0.35	0.05	0.09	159	3.09	0.2	0.43	0.002	0.7	0.21	10.3	0.35	4.35	1.36
1.1	0.37	1.08	45.2	33.2	428	6.85	5.58	0.48	0.11	8.94	0.31	0.09	0.1	82.3	5.13	0.45	0.78	bdl	0.28	0.2	20.2	0.65	7.83	1.9
nd	0.12	8.88	53.6	11.1	373	21.4	1.33	0.39	0.11	4.42	0.06	0.05	0.41	160	11.5	1.4	2.45	bdl	0.36	0.38	30.4	0.18	13.4	1.96
nd	0.23	13.2	63.3	11.9	298	16.3	2.66	0.48	0.11	3.81	0.16	0.04	0.59	167	7.77	0.99	1.72	bdl	0.34	0.59	20.6	0.31	10.3	1.96
nd	0.24	9.76	63.4	14.9	439	20.5	1.01	0.31	0.09	4.8	0.12	0.05	0.42	151	11.8	1.26	1.92	bdl	0.59	0.37	20.3	0.17	10.2	1.94
nd	0.23	17.5	107	15.8	150	22.9	1.55	0.36	0.14	5.73	0.11	0.06	0.86	215	7	1.5	2.33	bdl	0.12	0.58	27.5	0.56	16.2	2.52
nd	0.14	12.2	67.8	9.77	162	18.6	2.11	0.45	0.14	3.14	0.1	0.03	0.59	171	6.32	1.19	2.25	bdl	0.16	0.4	24.9	0.45	11.5	2.05
3.8	0.84	2.12	67.4	51.4	871	16.8	4.25	0.34	0.19	6.45	0.31	0.06	0.16	103	12.5	1.32	1.61	0.001	0.31	0.07	77.3	1.57	28.5	5.19
nd	0.11	2.7	43.5	8.47	322	16.2	2.19	0.18	0.06	2.55	0.25	0.03	0.21	128	7.31	1	1.43	bdl	0.17	0.32	40.3	0.59	8.72	3.55
2.5	0.64	2.28	75.8	51.2	133	7.33	6.18	0.25	0.1	3.92	0.67	0.05	0.1	145	12	0.49	0.78	0.014	0.34	0.35	32.8	0.65	7.84	5.41
0.5	0.41	1.57	88.2	33.3	710	17.7	3.31	0.15	0.1	5.18	0.26	0.05	0.11	111	12	1.33	1.95	bdl	0.22	0.1	28.4	0.6	13.7	5.94
1.2	0.37	1.16	47.9	30.3	989	15.2	4.61	0.23	0.12	5.41	0.36	0.06	0.08	95.1	12	1.28	1.69	0.011	0.26	0.06	32.9	1.05	13.5	4.82
2	0.55	1.86	87.1	40.9	167	12.7	5.48	0.19	0.11	5.51	0.26	0.06	0.09	117	14.9	1.19	0.95	0.012	0.35	0.17	31.8	0.6	12.5	5.75
2.9	0.32	1.89	175	24.4	110	13.5	4.54	0.23	0.1	4.52	0.52	0.05	0.1	430	12.3	1.18	0.88	0.026	0.42	0.32	38.1	0.61	15.5	3.94
nd	0.08	3.4	265	4.61	107	5.67	0.64	0.09	0.03	3.08	0.23	0.04	0.48	535	3.2	0.28	1.11	0.002	0.34	2.38	3.77	0.06	2	0.73
nd	0.15	4.11	68.8	10.8	450	17.4	2.36	0.23	0.12	6	0.35	0.07	0.42	139	8.92	1.43	2.2	0.003	0.19	0.63	16.2	0.48	12.8	2.68
1.5	0.32	3.28	28.2	26.6	719	16	3.74	0.21	0.14	5.79	0.49	0.07	0.22	113	11.3	1.4	1	0.005	0.35	0.21	34.3	1.26	19.7	3.76
1.8	0.27	1.62	833	22.1	102	12.1	3.71	0.26	0.07	6.39	0.27	0.08	0.08	2238	8.81	0.93	0.87	0.002	0.32	0.27	20.6	0.41	11.1	2.6
1.6	0.21	0.65	931	20.7	129	11.7	4.95	0.2	0.07	3.83	0.38	0.04	0.05	2244	9.4	0.71	1.09	bdl	0.3	0.2	17.2	0.34	9.49	2.04
1	0.19	1.61	146	14.2	594	6.5	3.02	0.28	0.1	3.86	0.36	0.06	0.12	243	6.08	0.44	0.77	0.007	0.23	0.18	17.4	0.51	6.38	1.96
0.3	0.24	0.8	368	17.3	737	5.85	2.5	0.18	0.08	3.41	0.29	0.04	0.04	890	6.1	0.35	0.57	0.003	0.24	0.22	13	0.79	5.56	2.82
nd	0.19	5.42	175	11.3	435	39.3	1.7	0.28	0.11	8.13	0.22	0.1	0.28	553	11.1	3.76	4.09	0.002	0.91	0.37	34.6	0.75	25.6	3.99
1.5	0.16	1.03	53.5	10.5	467	4.98	2.81	0.14	0.06	3.37	0.24	0.04	0.11	127	4.98	0.37	0.74	0.003	0.21	0.26	14.6	0.41	5.96	1.48
1	0.14	1.38	231	10.7	286	4.16	2.18	0.15	0.04	3.8	0.16	0.05	0.11	207	3.2	0.36	1.02	bdl	0.14	0.62	13	0.38	4.34	0.94
0.1	0.14	0.77	79.1	11.1	280	2.75	1.92	0.09	0.04	2.9	0.19	0.04	0.04	183	2.39	0.13	0.49	bdl	0.22	0.24	9.85	0.24	3.19	0.77
nd	0.17	6.71	125	14.1	537	19.2	1.58	0.26	0.09	5.05	0.28	0.06	0.58	346	11.4	1.5	2.38	bdl	0.4	0.37	23	0.67	24.6	5.47
1.4	0.15	0.3	99.8	14.1	204	2.01	1.52	0.06	0.03	2.17	0.15	0.02	0.01	149	1.24	0.13	0.63	bdl	0.11	0.12	7.04	0.18	2.64	0.9
2.9	0.12	0.62	55.9	10.5	123	6.75	1.77	0.14	0.05	3.8	0.19	0.04	0.03	179	3.77	0.5	0.61	0.001	0.19	0.12	12.7	0.3	7.2	1.84
2.7	0.17	0.53	96.8	14.1	598	4.41	1.76	0.28	0.04	7.98	0.16	0.1	0.03	247	2.36	0.3	0.64	bdl	0.12	0.33	9.93	0.2	3.95	1.21
nd	0.16	6.72	80	15.3	275	19.1	1.21	0.23	0.07	7.08	0.32	0.09	0.51	95.1	6.3	1.55	3.08	bdl	0.31	0.51	32.6	0.5	14.7	3.42
1.1	0.23	3.61	109	18	389	16.2	2.14	0.19	0.07	5.97	0.29	0.07	0.33	90.6	6.14	1.23	2.13	bdl	0.32	0.37	24.6	0.54	10.7	3.23
1.4	0.39	1.22	110	36.9	333	14.6	6.91	0.28	0.11	6.7	1.53	0.07	0.09	62.8	20.8	0.81	1.08	bdl	0.72	0.09	27.6	0.47	35.4	14.3
1.8	0.41	2.59	216	34.6	520	14.9	3.23	0.17	0.07	4.13	0.7	0.05	0.3	113	9.84	0.68	1.02	0.002	0.2	0.15	35	0.38	14.6	3.83
<1	0.18	2.89	39.9	18.9	557	12.4	4.85	0.17	0.11	5.8	0.47	0.05	0.3	58.3	7.96	0.87	1.38	bdl	0.22	0.24	15.9	0.46	15.9	3.32
1.3	0.17	2.12	30.8	13.1	358	7.11	2.03	0.16	0.05	4.68	0.64	0.06	0.2	72.3	6.51	1.02	1.15	bdl	0.64	0.31	22.9	0.35	15.1	2.55
2.3	0.28	0.81	6.73	24.8	131	6.51	2.15	0.24	0.1	4.82	0.31	0.06	0.04	30.8	8.72	0.43	0.54	bdl	0.41	0.05	21.8	0.34	9.42	2.64
1.2	0.3	1.19	10.2	23.5	783	9.92	2.36	0.2	0.07	4.37	0.39	0.06	0.1	43.7	8.57	0.71	1.3	bdl	0.78	0.12	24.3	0.42	12.3	3.37
1	0.15	1.08	10.7	14.9	580	6.41	2.5	0.13	0.06	4.1	0.37	0.05	0.08	34.6	5.77	0.46	0.69	bdl	0.16	0.18	17.3	0.25	5.95	1.84
1.2	0.32	1.55	9.02	24.4	580	11.9	1.97	0.25	0.1	4.49	0.33	0.05	0.12	50.6	6.7	0.84	1.44	0.001	0.35	0.11	40.6	0.65	10.9	3.55
1.5	0.26	1.43	13.9	19.8	449	9.08	2.13	0.24	0.09	4.54	0.34	0.06	0.09	47.6	9.44	0.66	0.84	0.001	0.45	0.1	34.9	0.57	11.9	2.78
0.7	0.37	1.33	24.7	21.2	685	12.5	3.78	0.36	0.08	4.6	0.46	0.06	0.08	44.8	10.8	0.82	0.86	0.006	0.35	0.09	23.1	0.37	9.23	2.72
nd	0.31	1.59	128	24.3	446	10.6	3.67	0.22	0.09	4.86	0.38	0.06	0.11	276	8.96	0.77	1.03	0.006	0.33	0.21	25.6	0.56	12.4	3.43
3.79	2.47	9.25	140	18.2	89.5	9.44	3.08	0.25	0.047	2.11	0.84	nd	1.13	159	3.71	0.62	1.08	<0.001[c]	0.163	0.47	15.1	0.79	5.84	2.43
8.3	1.3	14	110	8.4	36	3.7	2.2	0.22	0.031	1.1	0.92	nd	1	150	1.2	0.28	1.1	nd	0.1	0.63	7.8	0.97	3.3	2.4

of the kaolinite (1.18), because kaolinite and quartz are major minerals present; however, some coals have been found with a very low SiO_2/Al_2O_3 ratio, such as the late Pennsylvanian coals of the Jungar Basin situated to the south of and close to the Daqingshan coalfield, which is rich in boehmite (AlOOH) (Dai et al., 2006, 2008). The vertical variation of SiO_2/Al_2O_3 (Fig. 10) in the CP2 coal is consistent with the variation in mineralogical composition (Fig. 3).

The proportions of CaO, MgO, and P_2O_5 in the CP2 coal are high in comparison with those in other Chinese coals. The elevated CaO and MgO reflect the high proportion of carbonate minerals in the coal. The correlation coefficients among CaO, Fe_2O_3, MgO, and MnO are high (Table 7), confirming that these elements mainly occur in the carbonate minerals (dolomite and calcite).

The high P_2O_5 in the coal is attributed to gorceixite and fluorapatite. Although P_2O_5 is negatively correlated with SiO_2, Al_2O_3, and ash yield ($P\text{-}A_d = -0.25$, $P\text{-}SiO_2 = -0.33$, $P\text{-}Al_2O_3 = -0.02$; Table 7), P does not necessarily occur in the organic matter, because the bulk of the gorceixite occurs in samples with relatively low ash yields.

Most of the samples in which >1% anatase was identified by XRD also have high percentages of TiO_2. Samples A42, with a remarkably high normalized TiO_2 percentage of 9.69%, also has an unusually high percentage of anatase (4.1%) and a high inferred TiO_2 percentage (5.70%) when the minerals are converted to an ash equivalent. Similarly, Samples A14, A6, A5, and A3 also have high observed and inferred TiO_2 percentages.

Only bench sample A7 contains a small percentage of pyrite (Table 3) and also has a measureable pyritic sulfur concentration (Table 1).

The four zones of the CP2 coal described above based on mineral composition also show different major element abundances (Fig. 3).

Zones I and IV. Owing to the dominant clay minerals and trace amounts of diaspore (Table 3), the SiO_2 to Al_2O_3 ratio for samples A1–A11 and A40–A44 is high (Fig. 10), averaging 1.1 and 0.98, respectively.

Zone II. Al_2O_3 is the dominant oxide in samples A13 to A24. With the exception of A25 ($SiO_2/Al_2O_3 = 1.05$), the SiO_2/Al_2O_3 ratio in most benches of Zone II is very low, from 0.02 to 0.86, with an average of 0.43, consistent with the abundance of diaspore and boehmite in the mineral matter in this part of the coal seam. The P_2O_5 content in this zone is 0.31%, much higher than that in Zones I (0.04%), III (0.111%), and IV (0.024%). The proportions of CaO and Fe_2O_3 in this zone and Zone IV are high relative to Zones I and III (Fig. 10; Table 5). Samples A23 and A24, where the mineral matter contains significant proportions of gorceixite/goyazite (Fig. 3), also contain unusually high concentrations of P_2O_5, Ba and Sr (Fig. 10). This material, however, appears to be confined only to the one horizon within the seam section.

Zone III. Because less diaspore and gorceixite but more clay minerals are present in this zone than in Zone II (Fig. 3), the SiO_2/Al_2O_3 ratio is higher but the P_2O_5 content is lower than in Zone II (Fig. 10). Sample A28, with relatively abundant diaspore/boehmite, has a low SiO_2/Al_2O_3 ratio, similar to that of the underlying Zone II coal samples. A few low SiO_2/Al_2O_3 ratio values are also found in Zone III, and in Zone IV as well, but these are in samples that do not have particularly high diaspore or boehmite contents.

4.4.3. Affinity of the elements

Correlation of the element concentrations with ash yield may provide preliminary information on their organic or inorganic affinity (Eskanazy et al., 2010; Kortenski and Sotirov, 2002). Five groups (Groups 1 to 5) of elements from the present study can be classified according to their correlation coefficients with ash yield (Table 7).

Group 1 includes Al_2O_3, SiO_2, Na_2O, and Li, which are strongly correlated with ash yield ($r_{ash} = 0.7–1.0$). Silicon and Al are major constituents of the aluminosilicate minerals (kaolinite and illite). In addition, minerals including diaspore and gorceixite are the major carriers of Al in this coal. The correlation coefficient between ash yield and SiO_2 is 0.90 and that between ash yield and Al_2O_3 is 0.89. Both Li and Na_2O have high correlation coefficients with SiO_2 and Al_2O_3.

Group 2 includes elements with a lesser but still relatively high inorganic affinity (Table 7). Elements in this group (K_2O, Be, Ga, Rb, Cs, and W) are strongly correlated with ash yield, with correlation coefficients between 0.50 and 0.69. Elements in this group have high aluminosilicate affinity ($r_{Al–Si} = 0.5–0.69$). These lithophile elements are probably associated with diaspore and clay minerals rather than in gorceixite, because they have a high correlation coefficient with SiO_2 and Al_2O_3, but low or negative correlation coefficients with P_2O_5 (ranging from −0.15 to 0.02) and Ba (ranging −0.07 from to −0.22).

Group 3 includes TiO_2, Ge, Se, Nb, La, Ce, Pr, Nd, Gd, Ta, Pb, and Bi, which have correlation coefficients with ash yield varying from 0.34 to 0.49. Among these elements, TiO_2, Nb, La, Ce, Pr, Nd, Tb, and Pb have an aluminosilicate affinity, with correlation coefficients $r_{Al–Si}$ ranging from 0.35 to 0.49.

Group 4 includes CaO, Fe_2O_3, MgO, MnO, P_2O_5, F, Cl, Sc, V, Cr, Co, Ni, Cu, Zn, Sr, Y, Zr, Mo, Cd, In, Sn, Sb, Te, Ba, Sm, Eu, Tb, Dy, Ho, Er, Tm, Yb, Lu, Hf, Re, Hg, Tl, Th, and U. These elements have correlation coefficients with ash yield that range from −0.32 to 0.34, indicating either organic or inorganic affinities.

Group 5 includes only S. The sulfur has a strong negative correlation coefficient with ash yield (−0.67), indicating a dominant organic affinity (i.e. that the sulfur is mainly organic sulfur).

4.4.4. Geochemical associations

The elemental associations of the Adaohai coals were studied by cluster analysis. Five groups of elemental association were identified (Fig. 11), referred to as Groups A, B, C, D, and E.

Group A. This group includes the REE, as well as Be, Y, Se, Ga, Ge, Sc, In, Pb, Bi, Nb, Ta, TiO_2, W, Hg, Sb, Zr, Hf, Th, and U (Fig. 11). With the exceptions of Sb, Hf, Hg, Th, and U, the elements in this group have relatively high positive correlation coefficients with ash yield, ranging from 0.29 to 0.62 (Table 7). The correlation coefficients between the REEs (especially the HREEs) and other elements in this group (with the exceptions of Ta, W, Hg, Sb, and Zr; $r<0.5$) are relatively high. The correlation coefficients increase with the REE atomic number (Table 8). Correlation coefficients among the rare earth elements are all higher than 0.6. Most elements in Group A are lithophile elements that probably occur in aluminosilicate minerals. Note that there is a weak relation between Zr and Hf ($r = -0.05$), indicating that Zr and Hf have been fractionated in the coal, although the geochemical process is not clear.

Group B. This group includes the elements Sn-Te-Zn-Cd-V-As-Cr-Cu-Mo-Ni-Re. Elements in this group have correlation coefficients with ash yield ranging from −0.24 to 0.30. With the exception of Cu–Cd (0.71), Ni–Re (0.58), and V–Cr (0.67), the correlation coefficients between the pairs of elements in this association are lower than 0.45. The elements in this group are probably associated with unidentified traces of sulfide minerals.

Group C consists of ash yield, Na_2O, Al_2O_3, SiO_2, Li, K_2O, Rb, Cs, and Tl (Fig. 11). With the exception of Tl, the four oxides, Li, Rb, and Cs are strongly correlated with ash yield (Table 7). SiO_2 and Al_2O_3 are major constituents of the ash-forming minerals (clay minerals and diaspore), and Na_2O, Li, K_2O, Rb, Cs, and Li probably also occur in these minerals.

Group D includes P_2O_5, Ba, F, Sr, S, and Cl. Although all these elements have negative correlation coefficients with ash yield, with the exception of sulfur mainly occurring in the organic matter, the other elements occur in minerals (gorceixite and fluorapatite). The low correlation coefficients between these elements and ash are probably because the occurrences of authigenic gorceixite and fluorapatite do not correspond to the high ash zones.

Group E consists of four oxides Fe_2O_3, MnO, CaO, and MgO. The correlation coefficients between these oxides and ash yield are low, but those between each pair of these oxides are much higher (Table 7). These oxides are thought to occur mainly in the carbonate minerals (dolomite, calcite, and siderite) and were probably derived from magmatic hydrothermal fluids.

4.4.5. Elevated trace elements in the coal

4.4.5.1. Fluorine. Published literature shows that fluorine commonly occurs in minerals such as clays and fluorapatite, and less commonly in fluorite, tourmaline, topaz, amphiboles, and micas (Finkelman, 1995; Godbeer and Swaine, 1987; Lu, 1996; Swaine, 1990); in addition, fluorine also has an organic affinity (Bouška et al., 2000; McIntyre et al., 1985). The organic and silicate associations of fluorine in the coals from the Haerwusu Surface Mine in the Jungar Coalfield account for more than 90% of the total fluorine (Wang et al., 2011b).

Although the correlation coefficient between F and ash yield is −0.05, it does not indicate that fluorine has an organic affinity. The positive correlation coefficients of F–P_2O_5 (0.76) and F–Ba (0.98) show that the F largely occurs in gorceixite, and thus, as expected, F is enriched in Zone II (Fig. 10). Only a trace proportion of F occurs in fluorapatite, which is very low in the coal. SEM-EDX data (Table 4) show that the average F concentration in the gorceixite and fluorapatite is 1.21 and 4.11%, respectively. However, the F concentration in the diaspore is below the detection limit of the SEM-EDX (Table 4). The mode of occurrence of F in the CP2 coal is different to that in the Jungar coals, where F occurs in boehmite and the organic matter (Dai et al., 2008; Wang et al., 2011b).

4.4.5.2. Gallium. Gallium in coal is generally related to clay minerals (Chou, 1997; Finkelman, 1993; Ren et al., 2006). The Adaohai coals have a Ga content (mean 16.3 μg/g) close to that of the Haerwusu coals (18 μg/g; Dai et al., 2008), lower than that of the Heidaigou coals (mean 45 μg/g; Dai et al., 2006), but much higher than that of other

Table 6
Normalized percentages of major elements based on XRF analysis and inferred ash chemistry (normalized inorganic oxides) from XRD analysis (%).

Sample no.	SiO_2		Al_2O_3		CaO		Fe_2O_3		K_2O		MgO		Na_2O		P_2O_5		TiO_2	
	A	B	A	B	A	B	A	B	A	B	A	B	A	B	A	B	A	B
Roof-4	62.64	68.96	34.42	29.96	0.13	0	0.78	0.34	0.72	0.74	0.14	0	0.02	0	0.04	0	1.09	0
Roof-3	51.58	53.01	44.82	44.35	0.23	0	1.04	0	0.31	2.64	0.05	0	0.06	0	0.09	0	1.81	0
Roof-2	52.6	53.55	45.62	45.04	0.09	0	0.44	0	0.11	1.42	0	0	0.05	0	0.08	0	1.01	0
Roof-1	47.11	50.95	42.63	43.07	4.16	2.46	2.94	1.63	0.08	1.25	0.7	0.64	0.12	0	0.06	0	2.19	0
A44	42.25	43.16	42.75	39.45	8.63	8.98	2.55	4.57	0.05	0.32	0.99	3.53	0.16	0	0.12	0	2.48	0
A43	48.43	50.98	43.6	43.64	3.2	1.74	1.18	0.5	0.19	2.76	0.36	0.38	0.11	0	0.09	0	2.83	0
A42	23.03	28.08	24.05	24.06	21	11.28	15.21	20.18	0.14	1.17	6.48	9.52	0.09	0	0.16	0	9.69	5.7
A41	24.33	25.12	28.51	25.7	34.2	32.32	9.39	11.39	0.04	0.32	2.15	5.16	0.13	0	0.04	0	0.95	0
A40	42.6	42.8	43.22	42.7	7.92	8.62	2.74	2.74	0.08	0.28	0.75	2.12	0.16	0	0.14	0	2.34	0.75
A39-P	51.16	52.42	44.69	45.57	0.45	0	1.09	0	0.26	0.98	0.04	0	0.07	0	0.1	0	2.14	1.03
A38-P	50.77	51.95	44.29	45.23	0.76	0	1.73	0	0.39	1.68	0.15	0	0.07	0	0.11	0	1.71	1.14
A37-P	50.85	52.62	44.8	46.51	0.2	0	1.41	0	0.26	0.87	0.04	0	0.08	0	0.09	0	2.27	0
A36-P	51.13	52.37	44.79	45.79	0.16	0.08	1.61	0	0.41	1.57	0.07	0	0.08	0	0.11	0.19	1.62	0
A35-P	51.36	52.95	44.86	45.88	0.13	0	1.37	0	0.4	1.18	0.06	0	0.07	0	0.12	0	1.63	0
A34	48.79	51.49	44.92	46.65	1.49	0.55	1.78	0.6	0.09	0.24	0.31	0.47	0.14	0	0.19	0	2.27	0
A33-P	51.72	52.37	46.16	47.3	0.22	0	0.39	0	0.09	0.33	0.03	0	0.15	0	0.11	0	1.14	0
A32	22.73	25.32	25.39	25.2	26.83	18.04	15.14	18.99	0.08	0.74	7.88	11.72	0.08	0	0.18	0	1.54	0
A31	48.9	50.6	47.46	48.35	0.44	0	0.89	0.58	0.06	0.47	0.09	0	0.11	0	0.21	0	1.84	0
A30	49.29	48.34	47.12	50.74	0.57	0.26	0.79	0.36	0.05	0.3	0.08	0	0.11	0	0.15	0	1.84	0
A29	46.19	46.33	48.23	52.04	0.87	0.09	1.05	0	0.12	0.72	0.17	0	0.1	0	0.38	0.24	2.88	0.58
A28	28.31	33.52	58.83	56.44	4.9	4.15	2.73	2.62	0.22	0.74	0.75	1.67	0.12	0	1.42	0.37	2.68	0.48
A27-P	39.13	42.38	36.69	34.27	18.98	13.37	3.19	1.42	0.12	7.45	1.11	1.1	0.03	0	0.15	0	0.49	0
A26-P	49.73	49.57	45.97	46.6	1.01	0.56	0.64	0.5	0.16	1.39	0.07	0	0.13	0	0.11	0.12	2.17	1.26
A25	49.12	50.68	46.61	46.53	0.55	0.32	0.72	0.36	0.17	1.77	0.09	0	0.15	0	0.11	0	2.48	0.34
A24	15.71	13.56	69.68	76.43	2.54	1.51	1.89	4.1	0.25	0.94	0.26	0	0.1	0	6.67	3.45	2.87	0
A23	8.2	4.79	73.4	81.59	4.01	2.49	2.05	4.9	0.1	0	0.36	0	0.09	0	8.48	6.23	3.3	0
A22	37.88	36.9	44.23	45.47	10.56	8.96	2.92	4.1	0.1	1.4	1.71	3.05	0.15	0	0.71	0.13	1.71	0
A21	34.32	27.05	46.23	51.89	10.5	9.37	3.55	5.96	0.06	0.53	1.72	4.29	0.19	0	1.79	0.92	1.57	0
A20-P	39.26	29.56	56.97	67.1	0.75	0	0.67	0	0.27	3.34	0.13	0	0.06	0	0.54	0	1.34	0
A19	40.2	37.38	47.25	44.61	7.63	9.09	2.2	3.69	0.09	2.39	1.07	2.85	0.18	0	0.16	0	1.18	0
A18	35.35	30.88	44.33	44.71	15.83	16.97	1.53	2.64	0.13	2.77	0.97	2.04	0.13	0	0.28	0	1.43	0
A17	10.74	7.04	23.39	21.43	34.67	27.61	22.06	31.38	0.03	0	7.74	12.55	0.14	0	0.15	0	0.53	0
A16-P	40.38	37.44	53.55	54.69	1.25	0.43	1.74	0.54	0.51	6.58	0.36	0	0.06	0	0.4	0	1.74	0.33
A15	0.92	0	41.59	42.7	36.19	29.49	10.81	15.63	0.01	0	8.34	11.41	0.05	0	0.98	0	0.92	0.76
A14	1.91	0	67.51	72.93	6.69	4.32	14.92	18.69	0.06	0	2.87	2.62	0.08	0	0.96	0	4.78	1.44
A13	14.44	10.25	65.78	68.65	8.22	9.37	5.82	7.03	0.1	1.27	1	1.11	0.2	0	1.54	0.68	2.81	1.63
A12-P	51.42	52.88	46.73	45.85	0.37	0	0.24	0	0.26	1.27	0.05	0	0.09	0	0.09	0	0.75	0
A11	49.37	51.18	46.53	43.11	0.79	2.17	0.37	1.6	0.2	1.32	0.13	0.62	0.1	0	0.35	0	2.16	0
A10	47.21	46.78	45.27	46.5	4.37	5.55	0.49	0.37	0.19	0.43	0.08	0	0.1	0	0.42	0.36	1.86	0
A9	51.7	53.28	46.05	46.17	0.26	0.08	0.23	0	0.12	0.27	0.03	0	0.11	0	0.35	0.2	1.15	0
A8	51.94	53.38	45.57	44.4	0.23	0	0.31	0	0.18	2.22	0.06	0	0.08	0	0.08	0	1.56	0
A7	33.92	39.36	34.13	32.94	12.53	6.58	14.36	16.56	0.11	1.13	3.69	3.44	0.12	0	0.04	0	0.82	0
A6	47.72	49.56	43.55	45.29	2.08	1.91	1.45	1.31	0.09	0.42	0.18	0	0.07	0	0.04	0	4.8	1.53
A5	48.79	49.81	43.77	42.64	1.75	2.93	1.75	3.17	0.11	0.38	0.09	0	0.08	0	0.04	0	3.59	1.07
A4	50.85	53.03	44.87	45.24	0.47	0.26	1.02	0.72	0.09	0.28	0.09	0	0.08	0	0.04	0	2.48	0.46
A3	49.55	52.17	43.94	43.69	0.9	0.78	1.64	1.37	0.13	0.59	0.08	0	0.09	0	0.04	0	3.6	1.4
A2	51.06	53.06	45.12	44.75	0.58	0.59	1.15	1.16	0.08	0.44	0.03	0	0.1	0	0.05	0	1.82	0
A1	51.16	53.3	45.14	45.07	0.51	0.33	0.57	0.43	0.04	0.28	0.06	0	0.09	0	0.07	0	2.35	0.58

A, normalized percentages of major elements based on XRF analysis; B, Inferred ash chemistry (normalized inorganic oxides) from XRD analysis.

Chinese coals (6.6 μg/g; Dai et al., 2011). It can be deduced in the present case that Ga mainly occurs in inorganic association, including the clay minerals and diaspore, based on the positive correlations of Ga–ash ($r = 0.62$), Ga–Al ($r = 0.63$), and Ga–Si ($r = 0.65$). The mode of occurrence of Ga in the Adaohai coals is different to that of the Haerwusu coals (major carriers: organic matter, kaolinite, and boehmite) and that of the Heidaigou coals (boehmite). Although gallium may replace Zn in sphalerite (Sun et al., 2007; Swaine, 1990), the low-sulfur content, the negative correlation coefficient of Ga–S ($r = -0.51$), and the apparent absence of sphalerite indicate that Ga is not related to sulfide in the Adaohai coals.

4.4.5.3. Zirconium. The average concentration of Zr is 446 μg/g, which is much higher than that of common Chinese (89.5 μg/g; Dai et al., 2011) and world coals (36 μg/g; Ketris and Yudovich, 2009). The correlation coefficients of Zr–Al and Zr–Si are relatively high, 0.40 and 0.51, respectively, indicating that Zr occurs in association with the clay minerals. Zircon is, however, the major carrier of Zr in the Heidaigou and Haerwusu Surface Mines of the Jungar Coalfield (Dai et al., 2006, 2008).

4.4.5.4. Thorium. The average Th content of the CP2 coal (12.4 μg/g) is higher by a factor of 2 than that of common Chinese coals (5.84 μg/g; Dai et al., 2011), but slightly lower than that in the Heidaigou (17.8 μg/g) and Haerwusu coals (17 μg/g) (Dai et al., 2006, 2008). Thorium in the Heidaigou and Haerwusu coals mainly occurs in zircon, boehmite, and organic matter (Dai et al., 2006, 2008). Thorium in the Adaohai coals has high correlation coefficients with TiO_2 (0.67), Be (0.63), Sc (0.77), Y (0.62), Nb (0.83), Ta (0.77), Bi (0.66), and heavy REE (0.56–0.66), probably indicating the same source for these elements. The relatively low correlation coefficients of Th–Al_2O_3 (0.21), Th–SiO_2 (0.27), and Th–ash (0.23) indicate that Th may occur in accessory minerals in the coal and probably in the organic matter as well.

Thorium in the coal of the Adaohai Coalfield is thought to be mainly derived from detrital materials of the source region. The Middle Proterozoic moyite of the Yinshan Oldland is enriched in Th

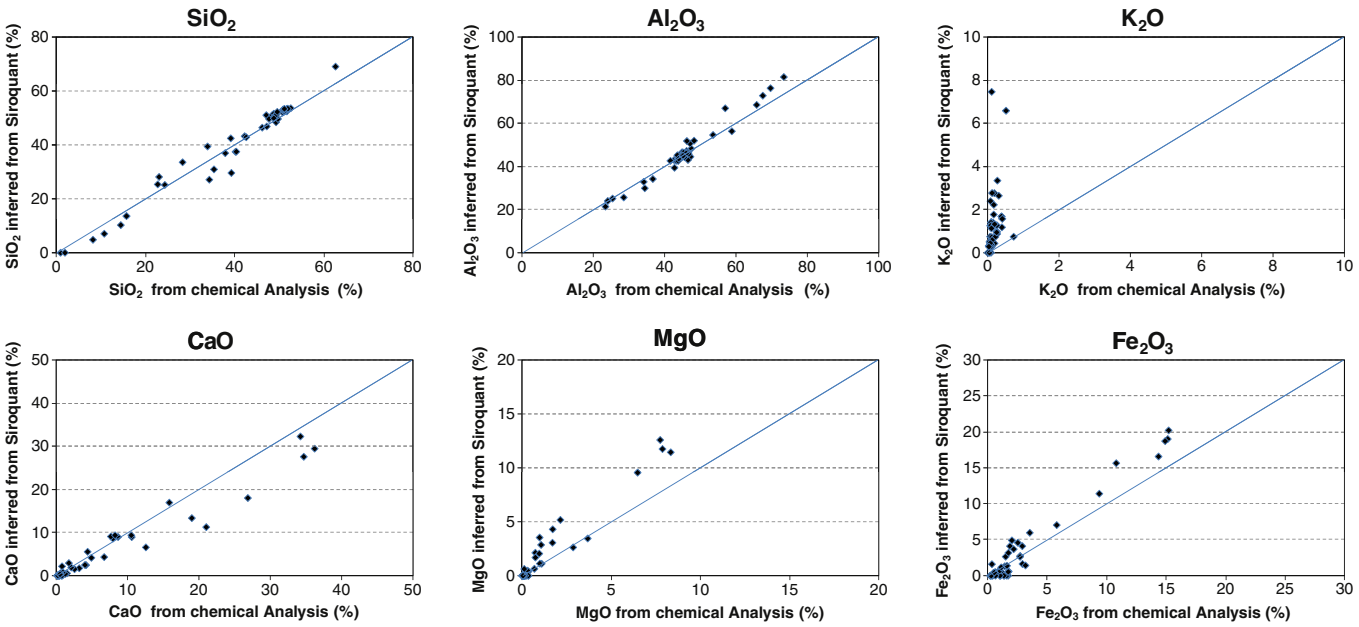

Fig. 9. Comparison of observed normalized oxide percentages from chemical analysis (x-axis) to oxide percentages for sample ash inferred from XRD analysis data (y-axis). The diagonal line in each plot indicates equality.

(Yan and Chi, 1997). The higher Th content in the Adaohai coals also suggests that the Th content is higher in the proximity of the sedimentary source region than further away. Thorium may not easily migrate in solution from the sediment-source region to the sedimentary basin because it can be hydrolyzed to $Th(OH)_4$, leading to in-situ deposition of Th.

4.4.5.5. Barium. The most probable carrier of Ba in coal is barite; however, barium can isomorphously substitute for Ca and K in ankerite, calcite, and feldspar, be adsorbed by clay minerals, or occur in the organic matter in low-rank coals (Bouška et al., 2000; Finkelman, 1995; Swaine, 1990). The Ba content in the Adaohai coals (276 μg/g on average) is not only higher than that of common Chinese (159 μg/g; Dai et al., 2011) and world coals (150 μg/g; Ketris and Yudovich, 2009), but is also higher than that in the Heidaigou (56 μg/g) and Haerwusu (41 μg/g) coals from the Jungar Coalfield. Note that Ba in benches A23 and A24 is very high, up to 2244 and 2238 μg/g, respectively (Fig. 10), reflecting the high proportion of gorceixite in these two benches (Fig. 3). SEM-EDX data show that Ba in the gorceixite has an average concentration of 16.19% (Table 4).

The high correlation coefficients of Ba–P_2O_5 (0.98) and Ba–Sr (0.98) confirm that gorceixite is one of the carriers of Ba in the coal. The relatively high correlation coefficient between Ba and S (0.45; Table 7), however, suggests that a portion of Ba may also occur in barite.

Because of the close relations among P_2O_5, F, Sr, and Ba, as described above, these elements have similar vertical distributions in the zones. They are all most abundant in Zone II (Fig. 10), where gorceixite and diaspore are enriched (Fig. 3).

4.4.5.6. Mercury. Despite its low level of abundance in coal, the concentration of mercury in coal is of growing concern due to its extremely toxic effects and its tendency for bioaccumulation through the food chain (Yudovich and Ketris, 2005). It is generally considered that Hg in coal is primarily present in pyrite (Hower et al., 2008), although some studies indicate that Hg also occurs in calcite and chlorite (Zhang et al., 2002), clausthalite (Hower and Robertson, 2003), kleinite and cinnabar (Brownfield et al., 2005).

The concentration of Hg in the Adaohai coals is high, averaging 0.33 μg/g. Mercury is one of the highly volatile elements in coal (Smith, 1987). Finkelman et al. (1998) found that Hg can be partially volatilized from coal at temperatures as low as about 150 °C and is completely volatilized at 550 °C. It seems that Hg inherent in coal may be easily driven off by magmatic heat. However, studies by Dai and Ren (2007), Finkelman et al. (1998), Golab and Carr (2004), and the present paper show that Hg is higher in altered coals near magmatic intrusions.

The low correlation coefficient of Hg-ash (0.12) indicates that Hg may have both organic and inorganic affinities. The enrichment of Hg in the altered coals indicates that, when the heat dissipated and temperatures dropped to ambient levels, Hg may have been re-deposited from the solutions that were derived from or had interacted with the cooling magma and were then adsorbed in the coal, rather than occurring in the sulfide minerals in coal (Finkelman et al., 1998). Mercury could also have been driven off from the organic component in the coal by magmatic heat and then re-deposited nearby, leading to enrichment of Hg in the altered coals.

4.4.5.7. Rare earth elements (REEs). The concentration of total REEs (from La to Lu) in the Adaohai coals varies from 41.7 to 429 μg/g and averages 156 μg/g, slightly higher than that in common Chinese (118 μg/g; Dai et al., 2011) and common world coals (60 μg/g; Ketris and Yudovich, 2009). The total REEs are high in Zones I, III, and IV, but low in Zone II (Fig. 10).

It has been reported that rare earth elements in coal are often positively correlated with ash yield and generally related to minerals, primarily clay minerals and phosphates (Chou, 1997; Dai et al., 2008; Finkelman, 1995). However, rare earth elements may also be partly associated with the organic matter in coal (Eskenazy, 1987a,b). The positive but not high correlation coefficients of REE–ash, REE–SiO_2, and REE–Al_2O_3 (Table 7) indicate that a proportion of the REEs is related to minerals in the Adaohai coals. However, the heavy REEs in coals from the Haerwusu mine have a stronger inorganic affinity than the LREEs (Dai et al., 2008). By contrast, the light rare earth elements (LREEs, from La to Eu) in the CP2 coal have higher positive coefficients with ash yield (Fig. 12). However, the heavy REEs (HREEs, from Gd to

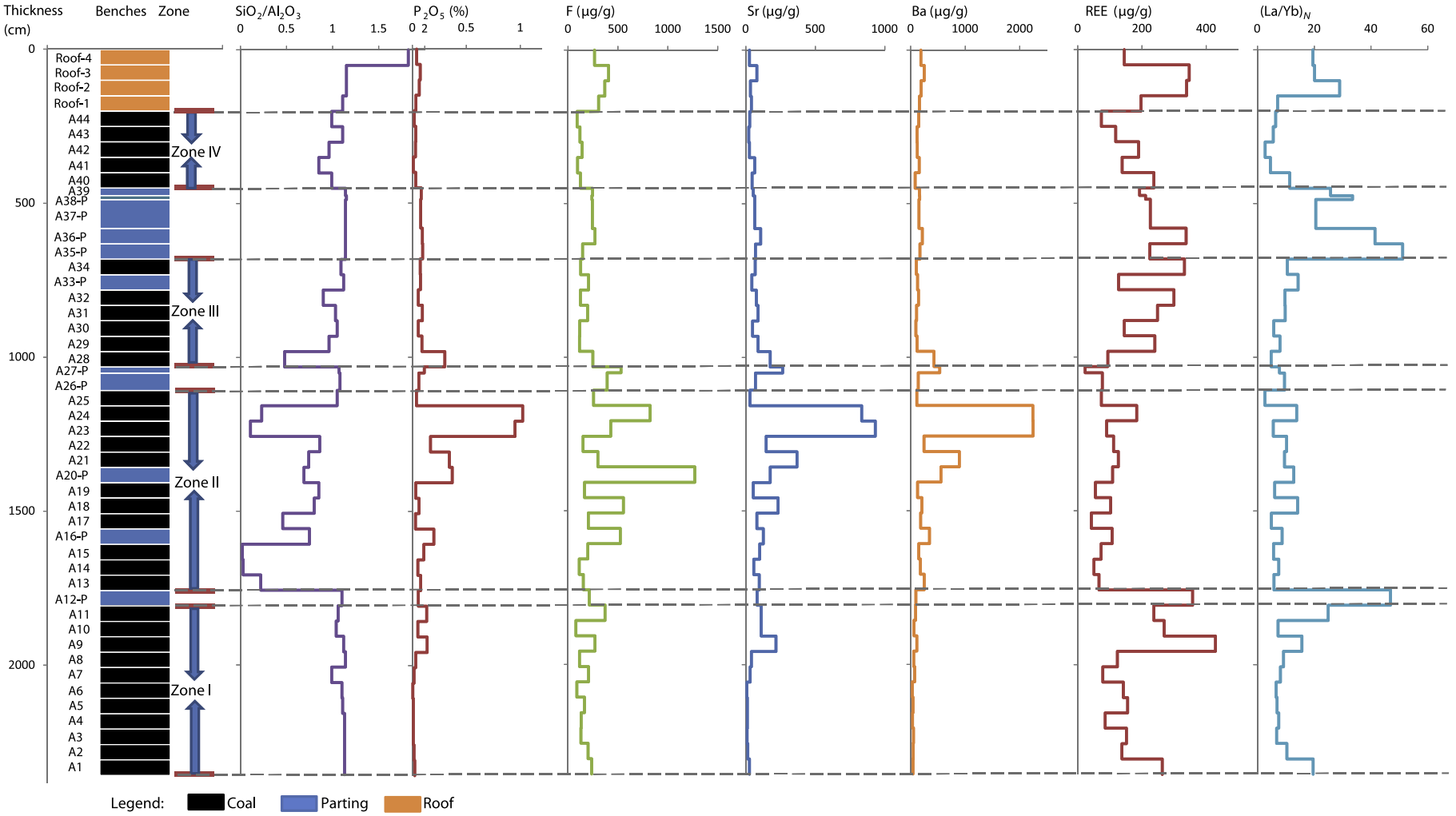

Fig. 10. Vertical variations of SiO_2/Al_2O_3 and some selected elements in the coal.

Table 7
Element affinities deduced from calculation of Pearson's correlation coefficients between the concentration of each element in the coal and ash yield or selected elements.

Correlation with ash yield
Group 1: r_{ash} = 0.7–1.0 Al_2O_3 (0.89), SiO_2 (0.90), Na_2O (0.86), Li (0.71)
Group 2: r_{ash} = 0.50–0.69 K_2O (0.64), Be (0.52), Ga (0.62), Rb (0.66), Cs (0.69), W (0.52)
Group 3: r_{ash} = 0.35–0.49 TiO_2 (0.39), Ge (0.40), Se (0.37), Nb (0.38), La (0.47), Ce (0.45), Pr (0.41), Nd (0.38), Gd (0.35), Ta (0.48), Pb (0.40), Bi (0.35)
Group 4: r_{ash} = −0.32–0.34 CaO (0.03), Fe_2O_3 (0.20), MgO (0.10), MnO (0.15), P_2O_5 (−0.25), F (−0.05), Cl (−0.1), As (0.16), Sc (0.32), V (0.30), Cr (0.29), Co (−0.18), Ni (0.22), Cu (−0.02), Zn (−0.24), Sr (−0.27), Y (0.31), Zr (0.34), Mo (0.13), Cd (0.04), In (0.32), Sn (0.09), Sb (0.14), Te (0.03), Ba (−0.32), Sm (0.33), Eu (0.29), Tb (0.32), Dy (0.32), Ho (0.31), Er (0.29), Tm (0.29), Yb (0.29), Lu (0.29), Hf (0.25), Re (0.10), Hg (0.12), Tl (0.07), Th (0.23), U (0.16)
Group 5: r_{ash} = S (−0.67)

Aluminosilicate affinity
r_{Al-Si} > 0.7 Na_2O, Li
r_{Al-Si} = 0.5–0.69 K_2O, Ga, Be, Rb, Cs, W
r_{Al-Si} = 0.35–0.49 TiO_2, Zr, Nb, La, Ce, Pr, Nd, Ta, Pb

Carbonate affinity
r_{Ca} > 0.7 Fe_2O_3 (0.83), MgO (0.87), MnO (0.80)
Correlation coefficient of other elements with Fe and Mg <0.32

Sulfate affinity
r_s > 0.7 no elements
r_s = 0.5–0.69 no elements
r_s = 0.35–0.49 Ba (0.45), Co (0.45)

Phosphate affinity
r_P > 0.7 F (0.76), Sr (0.98), Ba (0.98)
r_P = 0.5–0.69 no elements
r_P = 0.35–0.49 Cl (0.48), Co (0.44)

Correlation coefficients between selected elements
Al_2O_3–SiO_2 = 0.93; Fe_2O_3–MgO = 0.93; Fe_2O_3–MnO = 0.94; MgO–MnO = 0.79; Ga–Al_2O_3 = 0.63; Ga–SiO_2 = 0.65; F-Ba = 0.74; Zr-P = 0.31; P_2O_5–Al_2O_3 = −0.02; P_2O_5–SiO_2 = −0.33
Cl–P_2O_5 = 0.48; Cl–Ba = 0.42; Cl–F = 0.45; Cl–Sr = 0.36

Lu) are weakly correlated with the ash yield (Fig. 12), indicating that the HREEs have a stronger organic affinity than the LREEs, in accordance with the studies by Eskenazy (1987a,b) and Querol et al. (1995), but not completely consistent with the study by Eskenazy (1999).

The different modes of REE occurrence for the Adaohai and Haerwusu coals probably reflect the different sources of REE in the coals. A large portion of the REEs in the Haerwusu coals were derived from the overlying partings, which had been subjected to significant leaching by groundwater. Rare earth elements in the leachate were then absorbed by the organic matter. The LREEs in the partings of the Haerwusu coals are more prone to leaching by groundwater than the HREEs, leading to low REE contents and low LREE/HREE ratios in the partings but high REE contents and high LREE/HREE ratios in the underlying coal benches (Dai et al., 2008).

However, with the exception of the A26-P and A27-P partings of the CP2 coal, the partings and roof samples of the CP2 coal have higher REE contents, higher LREE/HREE ratios, and higher $(La/Yb)_N$ values than the underlying coal benches (Table 9; Fig. 10), sharply contrasting to the coals from the Haerwusu area and indicating that the partings were probably not subjected to groundwater leaching.

The cerium anomaly is expressed as Ce/Ce* whereby Ce concentration is either depleted or enriched in the samples relative to the other rare earth elements. The Ce/Ce* in the partings is lower than that in the underlying bench samples of the Adaohai coal (Table 9). However, the Haerwusu coals show the opposite cerium geochemical patterns, because Ce was oxidized to Ce^{4+} and precipitated in-situ during the leaching, leading to the generation of Ce-poor leachates from the Haerwusu partings. This may have caused the partings in the Haerwusu coals to have lower total REE contents, but higher Ce content and Ce/Ce* values than the underlying coal benches.

The high L/H (mean 8.13) ratio and $(La/Yb)_N$ value (mean 8.71) for the Adaohai coals (although lower than those of the partings) indicate that the coals are enriched in light REE and that the LREE–HREE have been highly fractionated. The lower values of $(Gd/Lu)_N$ than $(La/Sm)_N$ for both coal benches and partings indicate that the LREEs have been fractionated more than the HREEs.

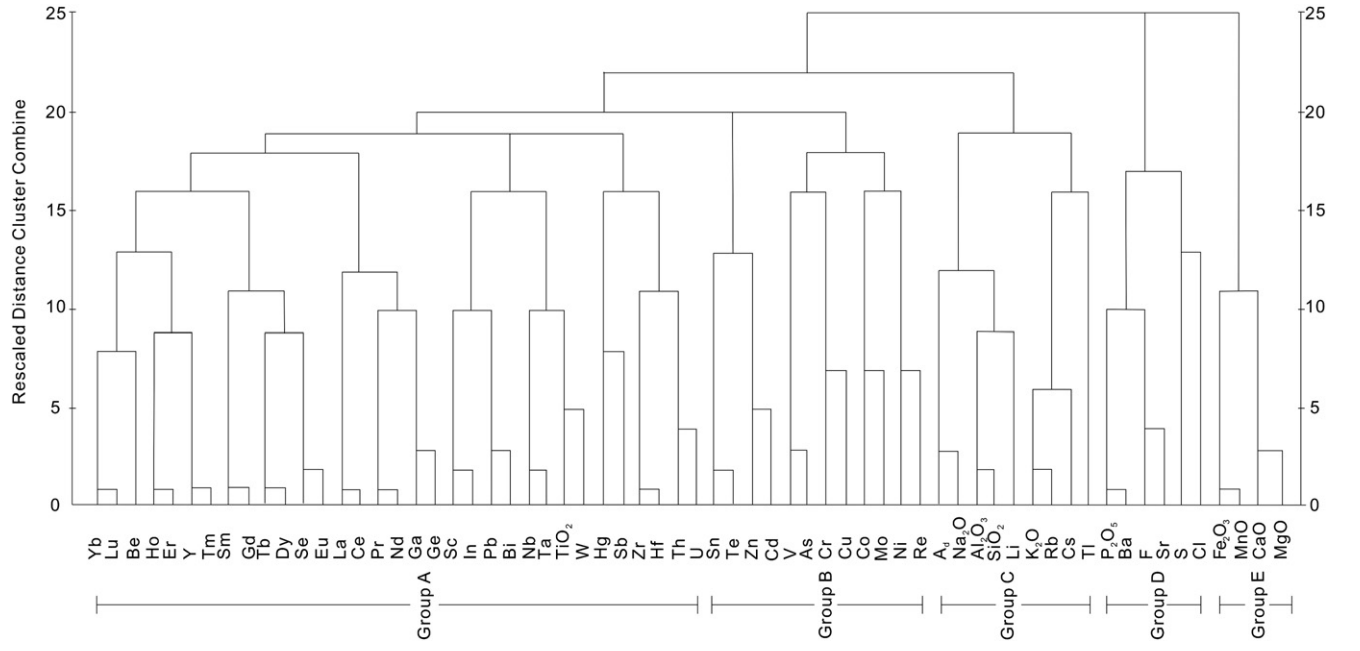

Fig. 11. Dendrogram produced by cluster analysis of analytical results on 33 samples.

Table 8
Correlation coefficients between REEs and selected elements.

REE	A_d	Al_2O_3	SiO_2	P	Sr	Ba	Be	Y	Se	Ga	Ge	Sc	In	Pb	Bi	Nb	Ta	TiO_2	W	Hg	Sb	Zr	Hf	Th	U
La	0.47	0.49	0.50	0.03	0.04	−0.07	0.64	0.60	0.61	0.73	0.80	0.30	0.28	0.42	0.19	0.32	0.21	0.19	0.32	0.01	0.33	0.09	0.26	0.22	0.36
Ce	0.45	0.45	0.49	−0.04	−0.01	−0.13	0.69	0.71	0.71	0.80	0.90	0.42	0.38	0.48	0.26	0.42	0.28	0.28	0.37	0.13	0.41	0.10	0.40	0.35	0.51
Pr	0.41	0.40	0.46	−0.03	−0.01	−0.11	0.67	0.70	0.69	0.80	0.95	0.46	0.39	0.49	0.26	0.47	0.32	0.35	0.36	0.21	0.42	0.09	0.46	0.40	0.53
Nd	0.37	0.36	0.41	−0.02	−0.01	−0.09	0.65	0.76	0.74	0.80	0.97	0.54	0.44	0.52	0.31	0.51	0.36	0.41	0.35	0.25	0.40	0.09	0.50	0.43	0.54
Sm	0.32	0.25	0.32	−0.06	−0.06	−0.11	0.62	0.86	0.84	0.77	0.96	0.68	0.56	0.62	0.43	0.53	0.39	0.47	0.31	0.32	0.43	0.07	0.58	0.52	0.58
Eu	0.28	0.22	0.22	0.16	0.14	0.14	0.56	0.88	0.89	0.68	0.83	0.79	0.67	0.70	0.59	0.58	0.49	0.57	0.34	0.33	0.23	0.02	0.59	0.54	0.47
Gd	0.34	0.26	0.32	−0.05	−0.07	−0.10	0.64	0.92	0.93	0.75	0.92	0.77	0.66	0.72	0.55	0.56	0.47	0.55	0.34	0.35	0.34	0.06	0.61	0.56	0.56
Tb	0.32	0.22	0.30	−0.07	−0.08	−0.10	0.67	0.95	0.95	0.73	0.84	0.82	0.74	0.76	0.63	0.57	0.48	0.54	0.36	0.38	0.38	0.07	0.65	0.64	0.63
Dy	0.31	0.20	0.29	−0.11	−0.13	−0.15	0.71	0.97	0.95	0.70	0.81	0.83	0.74	0.77	0.64	0.56	0.48	0.54	0.36	0.41	0.39	0.06	0.64	0.64	0.65
Ho	0.30	0.20	0.28	−0.09	−0.11	−0.13	0.73	0.99	0.95	0.71	0.79	0.83	0.74	0.74	0.62	0.56	0.49	0.52	0.37	0.40	0.42	0.04	0.65	0.63	0.68
Er	0.28	0.19	0.27	−0.11	−0.13	−0.16	0.75	0.99	0.94	0.70	0.77	0.82	0.75	0.75	0.62	0.58	0.50	0.51	0.37	0.40	0.43	0.02	0.67	0.65	0.70
Tm	0.28	0.20	0.26	−0.08	−0.09	−0.13	0.76	0.98	0.92	0.69	0.75	0.81	0.74	0.75	0.63	0.58	0.50	0.49	0.39	0.35	0.45	0.03	0.66	0.66	0.71
Yb	0.28	0.20	0.28	−0.09	−0.10	−0.15	0.77	0.97	0.91	0.71	0.77	0.79	0.71	0.73	0.58	0.58	0.48	0.49	0.38	0.37	0.45	0.02	0.66	0.64	0.70
Lu	0.28	0.23	0.29	−0.06	−0.07	−0.12	0.79	0.96	0.90	0.70	0.75	0.77	0.70	0.72	0.57	0.57	0.48	0.46	0.39	0.36	0.46	0.03	0.64	0.63	0.71

Although the ionic radii of the rare earth elements are similar, small differences in ionic radii among the REEs could lead to varying ability for isomorphous replacement in minerals (Liu and Cao, 1993; Taylor and Mclennan, 1985). The similarity in ionic radius between the HREEs and Sc^{3+} and Hf^{4+} usually results in Sc- and Hf-bearing minerals being relatively enriched in HREEs. The similarity in ionic radii between the LREEs and Sr^{2+} or Ba^{2+} also leads to Sr- or Ba-bearing minerals being relatively enriched in light REEs. This may be reason for the high correlation coefficients between LREE and Sr and Ba in the Haerwusu coals (Dai et al., 2008). The CP2 coals from the Adaohai Mine do not show such similarity, but have negative correlation coefficients between LREE and Sr, Ba, and P_2O_5 (Table 8), indicating that the REEs do not occur significantly in gorceixite in the coal. However, the HREEs in both the Adaohai and Haerwusu coals have positive correlation coefficients with Sc and Hf (Table 8).

5. Conclusions

The CP2 coal in the Adaohai Mine has a relatively higher coal rank (low volatile bituminous, $R_{o,\ ran} = 1.58\%$) than others in the basin, which is attributed to the influence of igneous intrusions during the Late Jurassic and Early Cretaceous Epochs. The coal has a medium-ash yield (25.1%) and a low sulfur content (0.78%), with the sulfur being mainly organic sulfur.

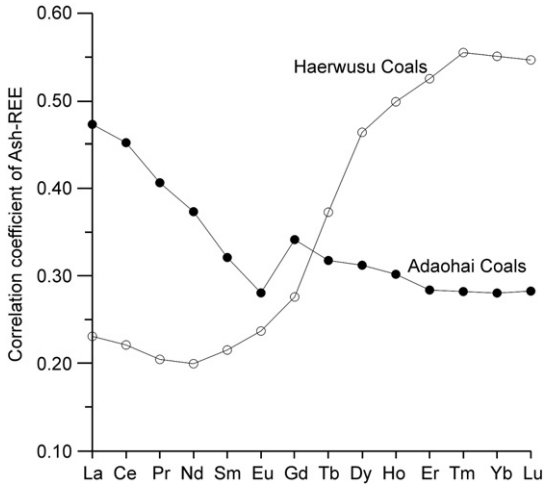

Fig. 12. Relation between REE-ash correlation coefficients and REE atomic number of coals from the Adaohai Mine and Haerwusu Surface Mine (Data for Haerwusu coals are from Dai et al., 2008).

Minerals in the CP2 coal include diaspore, boehmite, gorceixite, calcite, dolomite, siderite, clay minerals (kaolinite and ammonian illite), and trace amounts of anatase, fluorapatite, quartz, and pyrite. Based on mineral proportions in the coal benches, the CP2 coal may be divided into four Zones (I to IV) from bottom to top. The dominant mineral in Zones I and IV is kaolinite. Zones II and III are mainly composed of ammonian illite, diaspore, boehmite, gorceixite, calcite, dolomite, and siderite. The diaspore-, boehmite-, and gorceixite-forming materials were derived from oxidized bauxite in the weathered crust of the Benxi Formation in the sediment-source region and introduced during peat accumulation. Gorceixite may have formed earlier than diaspore, with the diaspore being derived from gibbsite that was subjected to dehydration by the heat of nearby igneous intrusions. The ammonian illite in the coal may have been formed at a relatively high temperature by interaction of kaolinite with nitrogen released from the organic matter in the coal during metamorphism caused by the igneous intrusion. The calcite and dolomite occur as epigenetic cell- and fracture-fillings, and were probably derived from igneous fluids.

The elements in the coal may be classified into five groups of association according to their modes of occurrence: Group A (REE-Be-Y-Se-Ga-Ge-Sc-In-Pb-Bi-Nb-Ta-TiO_2-W-Hg-Sb-Zr-Hf-Th-U), Group B (Sn-Te-Zn-Cd-V-As-Cr-Cu-Mo-Ni-Re), Group C (A_d-Na_2O-Al_2O_3-SiO_2-Li-K_2O-Rb-Cs-Tl), Group D (P_2O_5-Ba-F-Sr-S-Cl), and Group E (Fe_2O_3-MnO-CaO-MgO). Groups A and C include elements that are strongly correlated with ash yield, and most elements from the remaining three associations have negative or weak correlation coefficients with ash yield.

In comparison with common Chinese and world coals, the CP2 coal is enriched in CaO, MgO, P_2O_5, F, Ga, Zr, Ba, Hg, Pb, and Th, but has a lower SiO_2/Al_2O_3 ratio. The major carriers of CaO and MgO are the carbonate minerals. The P_2O_5, F, and Ba occur mainly in gorceixite and fluorapatite. The major carrier of Ga is diaspore and kaolinite. Mercury was probably derived from the igneous intrusion and distributed in both the organic matter and the minerals.

The light REEs are enriched in the coal and the LREEs and HREEs have been highly fractionated. The heavy REEs in the coals have a stronger organic affinity than the LREEs.

Acknowledgements

This research was supported by the National Science Fund for Distinguished Young Scholars (no. 40725008) and the National Natural Science Foundation of China (nos. 40930420 and 40831160520). Thanks are given to Editor Ralf Littke and two anonymous reviewers for their useful comments.

Table 9
Rare earth elements in coal benches and partings from the Adaohai Mine of the Daqingshan Coalfield (concentration of REE in μg/g; on whole-coal basis).

Sample	La	Ce	Pr	Nd	Sm	Eu	Gd	Tb	Dy	Ho	Er	Tm	Yb	Lu	REE	LREE	HREE	L/H	Eu/Eu*	Ce/Ce*	$(La/Yb)_N$	$(La/Sm)_N$	$(Gd/Lu)_N$
Roof-4	36.7	61.5	7.23	26.9	3.76	0.66	2.81	0.38	2	0.34	1.08	0.17	1.27	0.22	145	136.8	8.27	16.54	0.60	0.84	19.53	6.14	1.59
Roof-3	82.4	151	17.5	61.5	9.8	1.85	7.44	1.25	6.64	1.06	3.05	0.46	2.77	0.42	347	324.1	23.09	14.03	0.64	0.9	20.1	5.29	2.21
Roof-2	80	164	17.1	54.4	6.88	1.04	5.13	0.73	4.03	0.74	2.16	0.32	1.87	0.27	339	323.4	15.25	21.21	0.51	1	28.91	7.32	2.37
Roof-1	46.1	82.3	8.54	29.3	4.98	1.16	5.85	1.03	6.54	1.28	3.97	0.62	4.42	0.67	197	172.4	24.38	7.07	0.66	0.92	7.05	5.83	1.09
A44	15.4	29.1	3.23	12.7	2.65	0.55	2.44	0.46	2.68	0.52	1.77	0.25	1.62	0.25	73.6	63.6	9.99	6.37	0.65	0.93	6.42	3.66	1.22
A43	21.6	49.2	5.61	20	3.97	1.03	4.2	0.79	4.39	0.8	2.51	0.4	2.63	0.38	118	101.4	16.1	6.3	0.77	1.03	5.55	3.42	1.38
A42	19.4	69.9	10.5	44.3	9.15	2.46	9.24	1.54	9.27	1.66	4.96	0.78	4.84	0.71	189	155.7	33	4.72	0.81	1.13	2.71	1.33	1.62
A41	22.3	55.1	6.75	26.7	5.14	1.32	5.46	0.91	5.64	1.09	3.29	0.47	3.31	0.5	138	117.3	20.67	5.68	0.76	1.05	4.55	2.73	1.36
A40	55.3	105	10	37.2	6.54	1.5	5.82	1.06	6.2	1.16	3.33	0.54	3.29	0.5	237	215.5	21.9	9.84	0.73	0.98	11.36	5.32	1.45
A39-P	43	94.7	8.98	30.8	4.15	0.87	3.28	0.53	2.66	0.38	1.05	0.18	1.13	0.16	192	182.5	9.37	19.48	0.7	1.08	25.71	6.52	2.55
A38-P	56.5	86.8	11.8	38.1	5.21	1.26	4.4	0.65	2.91	0.5	1.35	0.18	1.14	0.18	211	199.7	11.31	17.65	0.78	0.76	33.49	6.83	3.04
A37-P	53.2	99	11.9	40.3	6.01	1.27	5.13	0.69	3.57	0.59	1.71	0.24	1.75	0.25	226	211.7	13.93	15.2	0.68	0.89	20.54	5.57	2.55
A36-P	87.6	144	17.9	61.1	8.55	1.86	6.58	0.93	4.55	0.64	1.79	0.24	1.43	0.21	337	321	16.37	19.61	0.73	0.81	41.4	6.45	3.9
A35-P	67.4	78.6	13.7	46.4	6.59	1.2	3.83	0.61	2.59	0.39	1.09	0.16	0.89	0.12	224	213.9	9.68	22.1	0.67	0.58	51.17	6.44	3.97
A34	80.8	145	13.1	45.2	9.13	2.41	9.99	1.82	10.3	1.84	5.34	0.88	5.2	0.85	332	295.6	36.22	8.16	0.77	0.96	10.5	5.57	1.46
A33-P	26.9	65.1	5.57	19.1	2.71	0.59	2.02	0.34	1.88	0.35	1.13	0.17	1.27	0.22	127	120	7.38	16.26	0.74	1.19	14.31	6.25	1.14
A32	70.5	127	12.1	44.1	9.45	2.15	9.22	1.52	9.27	1.75	5.07	0.81	4.9	0.77	299	265.3	33.31	7.96	0.7	0.95	9.72	4.7	1.49
A31	49.7	111	12	45	6.82	1.47	6.17	0.98	5.91	1.19	3.49	0.56	3.45	0.59	248	226	22.34	10.12	0.68	1.04	9.73	4.59	1.3
A30	26.3	60.9	7.08	26.4	4.45	1.02	4.81	0.81	4.86	0.97	2.94	0.53	3.1	0.47	145	126.2	18.49	6.82	0.67	1.03	5.73	3.72	1.27
A29	47.8	105	11.9	41.9	6.74	1.41	6.85	1.11	6.49	1.34	4.23	0.61	4.09	0.64	240	214.8	25.36	8.47	0.63	1.01	7.9	4.46	1.33
A28	18.8	33.5	4.16	17.4	3.38	0.86	3.77	0.62	3.9	0.75	2.65	0.42	2.65	0.42	93.3	78.1	15.18	5.14	0.73	0.86	4.79	3.5	1.12
A27-P	4.36	8.89	1.17	4.16	0.85	0.32	1.08	0.17	0.89	0.15	0.42	0.08	0.38	0.07	23	19.8	3.24	6.1	1.02	0.91	7.75	3.23	1.92
A26-P	20.5	33.4	3.13	9.3	1.67	0.41	1.91	0.37	2.16	0.39	1.3	0.19	1.45	0.21	76.4	68.4	7.98	8.57	0.7	0.89	9.55	7.73	1.13
A25	10.6	25.1	3.19	13.3	3.49	0.89	4	0.79	4.74	0.93	2.92	0.46	2.72	0.44	73.6	56.6	17	3.33	0.73	1.01	2.63	1.91	1.13
A24	44	73.9	8.88	33.2	4.98	1.72	5.31	0.78	4.39	0.77	2.26	0.35	2.15	0.35	183	166.7	16.36	10.19	1.02	0.84	13.83	5.56	1.89
A23	17.7	34.7	3.98	15.9	3.49	1.22	3.2	0.65	3.21	0.71	1.99	0.35	2.16	0.37	89.6	77	12.64	6.09	1.1	0.94	5.54	3.19	1.08
A22	26	50.9	5.4	15.7	2.35	0.56	2.51	0.44	2.72	0.53	1.64	0.26	1.71	0.24	111	100.9	10.05	10.04	0.7	0.96	10.27	6.96	1.3
A21	26.5	52.8	6.28	22.8	3.84	1.03	3.58	0.64	3.67	0.66	1.96	0.31	1.89	0.28	126	113.3	12.99	8.72	0.84	0.93	9.47	4.34	1.59
A20-P	28.8	47.8	4.92	15	2.16	0.52	2.35	0.4	2.3	0.44	1.38	0.25	1.52	0.23	108	99.2	8.87	11.18	0.7	0.87	12.8	8.39	1.27
A19	10.8	22.4	2.59	8.92	1.72	0.33	2	0.36	2.27	0.38	1.26	0.17	1.21	0.17	54.6	46.8	7.82	5.98	0.54	0.97	6.03	3.95	1.46
A18	24.5	46.1	5.16	15.9	1.95	0.42	2.15	0.35	2.15	0.39	1.24	0.21	1.17	0.19	102	94	7.85	11.98	0.62	0.92	14.15	7.91	1.41
A17	7.13	16	1.95	7.31	1.53	0.37	2.02	0.35	2.13	0.36	1.18	0.17	0.99	0.16	41.7	34.3	7.36	4.66	0.64	0.99	4.87	2.93	1.57
A16-P	24.8	46.1	4.95	16.7	2.66	0.47	2.93	0.48	2.89	0.55	1.79	0.27	1.93	0.27	107	95.7	11.11	8.61	0.51	0.93	8.68	5.87	1.35
A15	13.4	28.5	3.63	14.3	2.72	0.37	2.35	0.48	2.72	0.49	1.5	0.27	1.61	0.24	72.6	62.9	9.66	6.51	0.44	0.95	5.62	3.1	1.22
A14	11.8	20.2	2.36	8.17	1.7	0.27	1.61	0.26	1.54	0.31	0.98	0.19	1.06	0.16	50.6	44.5	6.11	7.28	0.49	0.85	7.52	4.37	1.25
A13	13.2	25.9	3.22	11.9	2.13	0.37	2.18	0.38	2.37	0.47	1.53	0.22	1.53	0.25	65.7	56.7	8.93	6.35	0.52	0.91	5.83	3.9	1.09
A12-P	118	180	14.4	32.3	2.36	0.46	2.78	0.34	1.97	0.41	1.45	0.25	1.7	0.31	357	347.5	9.21	37.73	0.55	0.88	46.9	31.47	1.12
A11	74	112	9.81	25.2	3.18	0.54	3.1	0.48	3.11	0.58	1.94	0.28	2.01	0.31	237	224.7	11.81	19.03	0.52	0.86	24.88	14.65	1.25
A10	50	122	13.5	45.6	8.25	1.27	6.7	1.28	7.67	1.49	4.58	0.75	4.66	0.75	269	240.6	27.88	8.63	0.51	1.09	7.25	3.81	1.11
A9	107	192	21.1	69.6	10.3	1.58	8.1	1.17	6.91	1.27	3.97	0.68	4.62	0.71	429	401.6	27.43	14.64	0.51	0.9	15.65	6.54	1.42
A8	27.2	53.3	5.92	20.5	3.08	0.57	3.02	0.6	3.44	0.67	2.05	0.31	2	0.35	123	110.6	12.44	8.89	0.56	0.95	9.19	5.56	1.07
A7	16.2	31.4	3.87	13.4	2.63	0.56	2.5	0.49	2.71	0.51	1.49	0.23	1.35	0.19	77.5	68.1	9.47	7.19	0.66	0.91	8.11	3.88	1.64
A6	26.6	59	7.13	25.6	4.82	0.91	4.75	0.82	4.88	0.92	2.86	0.43	2.73	0.43	142	124.1	17.82	6.96	0.57	0.99	6.58	3.47	1.38
A5	27.9	64.4	8.14	29.8	5.15	1.08	4.94	0.81	5.1	0.91	2.66	0.42	2.73	0.45	155	136.5	18.02	7.57	0.65	0.99	6.91	3.41	1.37
A4	21.9	33.6	3.48	12.2	2.37	0.53	2.43	0.42	3	0.57	1.86	0.29	1.98	0.31	84.9	74.1	10.86	6.82	0.67	0.83	7.47	5.82	0.98
A3	27.6	62.2	7.81	29	5.06	1.03	5	0.84	4.8	0.89	2.63	0.41	2.76	0.43	151	132.7	17.76	7.47	0.62	0.98	6.76	3.43	1.45
A2	32.2	56.3	6.33	22.4	3.8	0.91	4.19	0.71	4.57	0.79	2.35	0.32	2.1	0.36	137	121.9	15.39	7.92	0.69	0.88	10.36	5.33	1.45
A1	51.1	111	14.6	54.9	9.7	1.89	8.28	1.13	5.25	0.83	2.03	0.28	1.76	0.23	263	243.2	19.79	12.29	0.63	0.94	19.62	3.32	4.48
Av- Coal	33.19	66.19	7.42	26.56	4.72	1.05	4.6	0.78	4.61	0.86	2.62	0.41	2.61	0.41	156	139.1	16.91	8.13	0.67	0.96	8.71	4.56	1.44
Av- P	48.28	80.40	8.95	28.48	3.90	0.84	3.30	0.50	2.58	0.44	1.31	0.20	1.33	0.20	181	170.8	9.86	16.59	0.71	0.89	24.75	8.61	2.18
China [a]	22.5	46.7	6.42	22.3	4.07	0.84	4.65	0.62	3.74	0.96	1.79	0.64	2.08	0.38	117.7	102.8	14.86	6.92	0.59	0.90	7.31	3.48	1.52
World [b]	11	23	3.5	12	2	0.47	2.7	0.32	2.1	0.54	0.93	0.31	1	0.2	60.1	52.0	8.1	6.42	0.62	0.87	7.43	3.46	1.68

L/H, ratio of LREE vs. HREE; $Eu/Eu^* = 2Eu_N/(Sm_N + Gd_N)$; $Ce/Ce^* = 2Ce_N/(La_N + Pr_N)$; Av-Coal, average content of REEs in coal; Av-P, average content of REE in partings; [a], from Dai et al. (2011); [b], from Ketris and Yudovich (2009). The chondrite-normalizing values for the calculations of Eu/Eu*, Ce/Ce*, $(La/Yb)_N$, $(La/Sm)_N$, and $(Gd/Lu)_N$ are from Taylor and McLennan (1985).

References

Belkin, H.E., Tewalt, S.J., Hower, J.C., Stucker, J.D., O'Keefe, J.M.K., Tatu, C.A., Buia, G., 2010. Petrography and geochemistry of Oligocene bituminous coal from the Jiu Valley, Petroşani basin (southern Carpathian Mountains), Romania. International Journal of Coal Geology 82, 68–80.

Boudou, J.P., Schimmelmann, A., Ader, M., Mastalerz, M., Sebilo, M., Gengembre, L., 2008. Organic nitrogen chemistry during low-grade metamorphism. Geochimica et Cosmochimica Acta 72, 1199–1221.

Bouška, V., Pešek, J., Sýkorová, I., 2000. Probable modes of occurrence of chemical elements in coal. Acta Montana. Serie B, Fuel, Carbon, Mineral Processing, Praha 10 (117), 53–90.

Brownfield, M.E., Affolter, R.H., Cathcart, J.D., Johnson, S.Y., Brownfield, I.K., Rice, C.A., Zielinski, R.A., 2005. Geologic setting and characterization of coal and the modes of occurrence of selected elements from the Franklin coal zone, Puget Group, John Henry No. 1 mine, King county, Washington. International Journal of Coal Geology 63, 247–275.

Burger, K., Zhou, Y., Tang, D., 1990. Synsedimentary volcanic-ash-derived illite tonsteins in Late Permian coal-bearing formations of southwestern China. International Journal of Coal Geology 15, 341–356.

Cheng, D., Shen, F., Chai, D., 2001. Genetic attribute and geological significance of bauxite ores in Shanxi, China. Journal of Taiyuan University of Technology 32, 576–579 (in Chinese with English abstract).

Chou, C.-L., 1997. Abundances of sulfur, chlorine, and trace elements in Illinois Basin coals, USA. Proceedings of the 14th Annual International Pittsburgh Coal Conference & Workshop, Taiyuan, China, Sept. 23–27, 1997, Section 1, pp. 76–87.

Cressey, B.A., Cressey, G., 1988. Preliminary mineralogical investigation of Leicester low-rank coal. International Journal of Coal Geology 10, 177–191.

Dai, S., Chou, C.-L., 2007. Occurrence and origin of minerals in a chamosite-bearing coal of Late Permian age, Zhaotong, Yunnan, China. American Mineralogist 92, 1253–1261.

Dai, S., Ren, D., 2007. Effects of magmatic intrusion on mineralogy and geochemistry of coals from the Fengfeng-Handan Coalfield, Hebei, China. Energy & Fuels 21, 1663–1673.

Dai, S., Ren, D., Chou, C.-L., Li, S., Jiang, Y., 2006. Mineralogy and geochemistry of the No. 6 coal (Pennsylvanian) in the Jungar Coalfield, Ordos Basin, China. International Journal of Coal Geology 66, 253–270.
Dai, S., Li, D., Chou, C.-L., Zhao, L., Zhang, Y., Ren, D., Ma, Y., Sun, Y., 2008. Mineralogy and geochemistry of boehmite-rich coals: new insights from the Haerwusu Surface Mine, Jungar Coalfield, Inner Mongolia, China. International Journal of Coal Geology 74, 185–202.
Dai, S., Wang, X., Chen, W., Li, D., Chou, C.-L., Zhou, Y., Zhu, C., Li, H., Zhu, X., Xing, Y., Zhang, W., Zou, J., 2010. A high-pyrite semianthracite of Late Permian age in the Songzao Coalfield, southwestern China: mineralogical and geochemical relations with underlying mafic tuffs. International Journal of Coal Geology 83, 430–445.
Dai, S., Ren, D., Chou, C.-L., Finkelman, R.B., Seredin, V.V., Zhou, Y.P., 2011. Geochemistry of trace elements in Chinese coals: a review of abundances, genetic types, impacts on human health, and industrial utilization. International Journal of Coal Geology. doi:10.1016/j.coal.2011.02.003.
Daniels, E.J., Altaner, S.P., 1990. Clay mineral authigenesis in coal and shale from the Anthracite region, Pennsylvania. American Mineralogist 75, 825–839.
Daniels, E.J., Altaner, S.P., 1993. Inorganic nitrogen in anthracite from eastern Pennsylvania, U.S.A. International Journal of Coal Geology 22, 21–35.
Dewison, M.G., 1989. Dispersed kaolinite in the Barnsley Seam coal (UK): evidence for a volcanic origin. International Journal of Coal Geology 11, 291–304.
Eskanazy, G.M., Finkelman, R.B., Chattarjee, S., 2010. Some considerations concerning the use of correlation coefficients and cluster analysis in interpreting coal geochemistry data. International Journal of Coal Geology 83, 491–493.
Eskenazy, G.M., 1987a. Rare earth elements and yttrium in lithotypes of Bulgarian coals. Organic Geochemistry 11, 83–89.
Eskenazy, G.M., 1987b. Rare earth elements in a sampled coal from the Pirin Deposit, Bulgaria. International Journal of Coal Geology 7, 301–314.
Eskenazy, G.M., 1999. Aspects of the geochemistry of rare earth elements in coal: an experimental approach. International Journal of Coal Geology 38, 285–295.
Finkelman, R.B., 1993. Trace and minor elements in coal. In: Engel, M.H., Macko, S.A. (Eds.), Organic Geochemistry. Plenum, New York, pp. 593–607.
Finkelman, R.B., 1995. Modes of occurrence of environmentally sensitive trace elements in coal. In: Swaine, D.J., Goodarzi, F. (Eds.), Environmental Aspects of Trace Elements in Coal. Kluwer Academic Publishing, Dordrecht, pp. 24–50.
Finkelman, R.B., Stanton, R.W., 1978. Identification and significance of accessory minerals from a bituminous coal. Fuel 57, 763–768.
Finkelman, R.B., Bostick, N.H., Dulong, F.T., Senftle, F.E., Thorpe, A.N., 1998. Influence of an igneous intrusion on the inorganic geochemistry of a bituminous coal from Pitkin County, Colorado. International Journal of Coal Geology 36, 223–241.
Godbeer, W.C., Swaine, D.J., 1987. Fluorine in Australian coals. Fuel 66, 794–798.
Golab, A.N., Carr, P.F., 2004. Changes in geochemistry and mineralogy of thermally altered coal, Upper Hunter Valley, Australia. International Journal of Coal Geology 57, 197–210.
Han, D., Ren, D., Wang, Y., Jin, K., Mao, H., Qin, Y., 1996. Coal Petrology of China. Publishing House of China University of Mining and Technology, Xuzhou, pp. 98–168 (in Chinese with English abstract).
Harvey, R.D., Ruch, R.R., 1986. Mineral matter in Illinois and other US coals. In: Vorres, K.S. (Ed.), Mineral Matter in Coal Ash and Coal: American Chemical Society Symposium Series, 301, pp. 10–40.
Hower, J.C., Robertson, J.D., 2003. Clausthalite in coal. International Journal of Coal Geology 53, 219–225.
Hower, J.C., Campbell, J.L., Teesdale, W.J., Nejedly, Z., Robertson, J.D., 2008. Scanning proton microprobe analysis of mercury and other trace elements in Fe-sulfides from a Kentucky coal. International Journal of Coal Geology 75, 88–92.
Jia, B., Wu, Y., 1995. The provenance and stratigraphic significance of volcanic event layers in the Late Paleozoic coal measures from Daqingshan, Inner Mongolia. Journal of Geology & Mineral Resources of North China 10, 203–213 (in Chinese with English abstract).
Kalaitzidis, S., Siavalas, G., Skarpelis, N., Araujo, C.V., Christanis, K., 2010. Late Cretaceous coal overlying karstic bauxite deposits in the Parnassus-Ghiona Unit, Central Greece: coal characteristics and depositional environment. International Journal of Coal Geology 81, 211–226.
Kalkreuth, W., Holz, M., Mexias, A., Balbinot, M., Levandowski, J., Willett, J., Finkelman, R.B., Burger, H., 2010. Depositional setting, petrology and chemistry of Permian coals from the Paraná Basin: 2. South Santa Catarina Coalfield, Brazil. International Journal of Coal Geology 84, 213–236.
Ketris, M.P., Yudovich, Y.E., 2009. Estimations of Clarkes for carbonaceous biolithes: world average for trace element contents in black shales and coals. International Journal of Coal Geology 78, 135–148.
Kisch, H.J., Taylor, G.H., 1966. Metamorphism and alteration near an intrusive-coal contact. Economic Geology 61, 343–361.
Kortenski, J., 1992. Carbonate minerals in Bulgarian coals with different degrees of coalification. International Journal of Coal Geology 20, 225–242.
Kortenski, J., Sotirov, A., 2002. Trace and major element content and distribution in Neogene lignite from the Sofia Basin, Bulgaria. International Journal of Coal Geology 52, 63–82.
Koukouzas, N., Ward, C.R., Li, Z., 2010. Mineralogy of lignites and associated strata in the Mavropigi field of the Ptolemais Basin, northern Greece. International Journal of Coal Geology 81, 182–190.
Kwiecinska, B.K., Hamburg, G., Vleeskens, J.M., 1992. Formation temperatures of natural coke in the Lower Silesian coal basin, Poland: evidence from pyrite and clays by SEM-EDX. International Journal of Coal Geology 21, 217–235.
Liang, S., Ren, D., Wang, S., Yao, G., 1997. Study of Al-hydrates in clay partings within the Permo-Carboniferous coal-bearing strata in North China. Scientia Geologica Sinica 32, 478–485 (in Chinese with English abstract).
Liu, Y., Cao, L., 1993. Elemental Geochemistry. Geological Publishing House, Beijing. (in Chinese).
Loughnan, F.C., Goldbery, R., 1972. Dawsonite and analcite in the Singleton Coal Measures of the Sydney Basin. American Mineralogist 57, 1437–1447.
Lu, B., 1996. Occurrences of fluorine and chlorine in Chinese coals. Coal Geology & Exploration 24 (1), 9–12 (in Chinese with English abstract).
Mackowsky, M.Th., 1968. Mineral matter in coal. In: Murchison, D.G., Westoll, T.S. (Eds.), Coal and Coal-Bearing Strata. Oliver and Boyd, London, pp. 309–321.
McIntyre, N.S., Martin, R.R., Chauvin, W.J., Winder, C.G., Brown, J.R., MacPhee, J.A., 1985. Studies of elemental distributions within discrete coal macerals: use of secondary ion mass spectrometry and X-ray photoelectron spectroscopy. Fuel 64, 1705–1711.
Nieto, F., 2002. Characterization of coexisting NH4- and K-micas in very low-grade metapelites. American Mineralogist 87, 205–216.
Palmer, C.A., Lyons, P.C., 1996. Selected elements and major minerals from bituminous coal as determined by INAA: implications for removing environmentally sensitive elements from coal. International Journal of Coal Geology 32, 151–166.
Permana, A., Ward, C.R., Li, Z., Gurba, L.W., Davison, S., 2010. Mineral matter in the high rank coals of the South Walker Creek area, northern Bowen Basin. In: Beeston, J.W. (Ed.), Proceedings of Bowen Basin Symposium – Back in (the) Black, Geological Society of Australia Coal Geology Group and Bowen Basin Geologists Group, Mackay, Queensland, 6–8 October, 2010, pp. 27–34.
Querol, X., Fernandez-Turiel, J.L., Lopez-Soler, A., 1995. Trace elements in coal and their behaviour during combustion in a large power station. Fuel 74, 331–343.
Querol, X., Whateley, M.K.G., Fernandez-Turiel, J.L., Tuncali, E., 1997. Geological controls on the mineralogy of the Beypazari lignite, central Anatolia, Turkey. International Journal of Coal Geology 33, 255–271.
Rao, P.D., Walsh, D.E., 1997. Nature and distribution of phosphorus minerals in Cook Inlet coals, Alaska. International Journal of Coal Geology 33, 19–42.
Ren, D., Zhao, F., Dai, S., Zhang, J., Luo, K., 2006. Geochemistry of Trace Elements in Coal. Science Press, Beijing. 556 pp. (in Chinese with English abstract).
Rietveld, H.M., 1969. A profile refinement method for nuclear and magnetic structures. Journal of Applied Crystallography 2, 65–71.
Ruan, C.-D., Ward, C.R., 2002. Quantitative X-ray powder diffraction analysis of clay minerals in Australian coals using Rietveld methods. Applied Clay Science 21, 227–240.
Seredin, V., Finkelman, R.B., 2008. Metalliferous coals: a review of the main genetic and geochemical types. International Journal of Coal Geology 76, 253–289.
Seredin, V.V., Shpirt, M.Y., 1995. Metalliferous coals: a new potential source of valuable trace elements as by-products. In: Pajares, Tascon (Eds.), Coal Science (Proceedings ICCS '95). Elsevier Science B. V. II, pp. 1649–1652.
Smith, I.M., 1987. Trace Elements from Coal Combustion: Emissions. International Energy Agency, London, U.K.. IEACRr01, 87 pp.
Sun, Y., Lin, M., Qin, P., Zhao, C., Jin, K., 2007. Geochemistry of the barkinite liptobiolith (Late Permian) from the Jinshan Mine, Anhui Province, China. Environmental Geochemistry and Health 29, 33–44.
Swaine, D.J., 1990. Trace Elements in Coal. Butterworths, London. 270 pp.
Taylor, J.C., 1991. Computer programs for standardless quantitative analysis of minerals using the full powder diffraction profile. Powder Diffraction 6, 2–9.
Taylor, S.R., McLennan, S.M., 1985. The Continental Crust: Its Composition and Evolution. Blackwell, London. 312 pp.
Wang, S., 1982. Spore and pollen in the Late Carboniferous and Early Permian coals from Yaogou mine of Junger, Inner Mongolia, China. Journal of China Coal Society 7 (2), 36–44 (in Chinese).
Wang, S. (Editor in Chief), 1996. Coal Accumulation and Coal Resources Evaluation of Ordos Basin, China. China Coal Industry Publishing House, Beijing, p. 437 (in Chinese with English abstract).
Wang, X., 2009. Geochemistry of Late Triassic coals in the Changhe Mine, Sichuan Basin, southwestern China: evidence for authigenic lanthanide enrichment. International Journal of Coal Geology 80, 167–174.
Wang, S., Ge, L., 2007. Geochemical characteristics of rare earth elements in kaolin of coal-bearing strata from the Daqingshan coalfield. Coal Geology & Exploitation 35 (1), 1–5 (in Chinese with English abstract).
Wang, X., Dai, S., Ren, D., Yang, J., 2011a. Mineralogy and geochemistry of Al-hydroxide/oxyhydroxide minerals-bearing coals of the Late Paleozoic age from the Weibei coalfield in southeastern Ordos Basin, China. Applied Geochemistry 26, 1086–1096.
Wang, X., Dai, S., Sun, Y., Li, D., Zhang, W., Zhang, Y., Luo, Y., 2011b. Modes of occurrence of fluorine in the Late Paleozoic No. 6 coal from the Haerwusu Surface Mine, Inner Mongolia, China. Fuel 90, 248–254.
Ward, C.R., 1974. Isolation of mineral matter from Australian bituminous coals using hydrogen peroxide. Fuel 53, 220–221.
Ward, C.R., 1978. Mineral matter in Australian bituminous coals. Proceedings, Australasian Institute of Mining and Metallurgy 267, 7–25.
Ward, C.R., 1989. Minerals in bituminous coals of the Sydney Basin (Australia) and the Illinois Basin (U.S.A.). International Journal of Coal Geology 13, 455–479.
Ward, C.R., 2002. Analysis and significance of mineral matter in coal seams. International Journal of Coal Geology 50, 135–168.
Ward, C.R., Christie, P.J., 1994. Clays and other minerals in coal seams of the Moura-Baralaba area, Bowen Basin, Australia. International Journal of Coal Geology 25, 287–309.
Ward, C.R., Warbrooke, P.R., Roberts, F.I., 1989. Geochemical and mineralogical changes in a coal seam due to contact metamorphism, Sydney Basin, New South Wales, Australia. International Journal of Coal Geology 11, 105–125.
Ward, C.R., Corcoran, J.F., Saxby, J.D., Read, H.W., 1996. Occurrence of phosphorus minerals in Australian coal seams. International Journal of Coal Geology 31, 185–210.

Ward, C.R., Spears, D.A., Booth, C.A., Staton, I., Gurba, L.W., 1999. Mineral matter and trace elements in coals of the Gunnedah Basin, New South Wales, Australia. International Journal of Coal Geology 40, 281–308.
Ward, C.R., Matulis, C.E., Taylor, J.C., Dale, L.S., 2001. Quantification of mineral matter in the Argonne Premium Coals using interactive Rietveld-based X-ray diffraction. International Journal of Coal Geology 46, 67–82.
Yan, M., Chi, Q., 1997. Geochemcial Compositions of Earth Crust and Rocks in Eastern China. Science Press, Beijing, pp. 1–292 (in Chinese).
Yudovich, Ya.E., Ketris, M.P., 2005. Mercury in coal: a review. Part 1. Geochemistry. International Journal of Coal Geology 62, 107–134.
Zhang, B., 1984. Some problems on the origin of carboniferous bauxite deposites in central Guizhou. Geological Review 30, 553–560 (in Chinese with English abstract).
Zhang, H., Zhou, C., Guo, M., Jia, B., 2000. The effect of depositional environments on the alteration of volcanic ashes — a case study of the Late Paleozoic coal-bearing strata in Daqingshan Coalfield. Acta Sedimentologica Sinica 18, 515–520 (in Chinese with English abstract).
Zhang, J., Ren, D., Zheng, C., Zeng, R., Chou, C.-L., Liu, J., 2002. Trace element abundances in major minerals of Late Permian coals from southwestern Guizhou Province, China. International Journal of Coal Geology 53, 55–64.
Zhong, R., Chen, F., 1988. Coal-bearing Construction in the Daqingshan Coalfield. Geological Press, Beijing, p. 64 (in Chinese with English abstract).
Zhong, R., Sun, S., Chen, F., Fu, Z., 1995. The discovery of Rhyo-tuffite in the Taiyuan Formation and stratigraphic correlation of the Daqingshan and Datong Coalfield. Acta Geoscientia Sinica. 3, pp. 291–301 (in Chinese with English abstract).
Zhou, C., Jia, B., 2000. Analysis of the Late Paleozoic Conglomerates from Daqingshan Coalfield in Inner Mongolia. Journal of Taiyuan University of Technology 31, 498–504 (in Chinese with English abstract).